Environmental processes in Rano Aroi (Easter Island) peat geochemistry forced by climate variability during the last 70 kyr

Margalef, O. [(1)], Martínez Cortizas, A. [(2)], Kylander, M. [(3)], Pla-Rabes, S. [(4,5)], Cañellas-Boltà, N.[(6,7)], Pueyo, J.J.[(7)], Sáez, A. [(7)], Valero-Garcés, B. L. [(8)], Giralt, S. [(1)]

[(1)] Institute of Earth Sciences Jaume Almera (ICTJA-CSIC), Sedimentary Geology and Geohazards, Lluís Solé i Sabarís s/n, E-08028 Barcelona, Spain (omargalefgeo@gmail.com)

[(2)] Departmento de Edafoloxía e Química Agrícola, Fac. de Bioloxía – Campus Vida, E-15782 Santiago, Spain

[(3)] Department of Geological Sciences and the Bolin Centre for Climate Research, Stockholm University, SE 10961 Stockholm, Sweden

[(4)] Ecological Research Center and Forestry Applications (CREAF). Campus de Bellaterra (UAB) 08193 Cerdanyola del Vallès, Barcelona. Spain.

[(5)] Advanced Studies Center of Blanes (CEAB-CSIC). C/ D'accés a la Cala St. Francesc, 14. Blanes. Girona. E-17300 Spain.

[(6)] Laboratory of Palynology and Paleoecology, Botanic Institute of Barcelona (IBB-CSIC-ICUB), Spain

[(7)] Faculty of Geology, Universitat de Barcelona, Martí i Franquès s/n, E-08028 Barcelona, Spain

[(8)] Instituto Pirenaico de Ecología (IPE-CSIC). Avda. de Montañana, 1005. 50059 Zaragoza, Spain

ABSTRACT

We analyze the geochemistry of Rano Aroi mire record (Easter Island) using bulk peat composition (C, N, S) and stable isotopes ($\delta^{13}C$, $\delta^{15}N$, $\delta^{34}S$) and major, minor and trace elemental composition obtained by ICP-AES (Al, Ti, Zr, Sc, V, Y, Fe, Mn, Th, Ba, Ca, Mg and Sr). Peat geochemistry and the pollen record are used to reconstruct the environmental changes during the last 70 kyr BP. Principal component analysis on ICP-AES data revealed that three main components account for the chemical signatures of the peat. The first component, characterized by lithogenic elements (combined signal of V, Al, Sc, Y, Cr, Cd, Ti, Zr and Cu), evidences long-term changes in the basal fluxes of mineral material into the mire. This component, in combination with stable isotopes and pollen data suggests a link between soil erosion and vegetation cover changes in the Rano Aroi watershed. The second component is identified by the signal of Fe, Mn, Th, Ba, Zr and Ti, and is indicative of strong runoff events during enhanced precipitation periods. The third component (tied mainly to Ca, Sr and Mg) reflects a strong peat oxidation event that occurred during an arid period with more frequent droughts, sometime between 39 and 31 kyr BP. Correlation coefficients and a multiple regression model (PCR analysis) between peat organic chemistry and the principal components of ICP-AES analysis were calculated. Isotope chemistry of the peat organic matter further contributes to define Rano Aroi environmental history: $\delta^{13}C$ data corroborates a vegetation shift documented by the palynological record from C_4 to C_3 between 55 and 45 kyr cal BP; the $\delta^{15}N$ record identifies periods of changes in mire productivity and denitrification processes, while the $\delta^{34}S$ peat signature indicates a marine origin of S and significant diagenetic cycling. The geochemical and environmental evolution of Rano Aroi mire is coherent with the regional climatic variability and suggests that climate was the main forcing in mire evolution during the last 70 kyr BP. The coupling

of geochemical and biological proxies improves our ability to decipher depositional processes in tropical and subtropical peatlands and to use these sequences for paleoenvironmental and paleoclimate reconstructions.

1. INTRODUCTION

Peatlands are paleoenvironmental archives capable of registering atmospheric, hydrological and ecological changes in the past (Jackson and Charman, 2010). Researchers have traditionally studied peat accumulation and decay dynamics (Clymo, 1984), and attempted to understand the contribution of these organic soils to the global carbon cycle (Gorham, 1991), as well as to reconstruct paleoecological changes using macrofossils, pollen (Barber et al., 2003; Birks and Birks, 2006) and charcoal remains (Whitlock and Larsen, 2001). In more recent times, inorganic geochemical proxies from peat sequences have increasingly been used to obtain high-resolution climatic and environmental reconstructions. For example, wind regime variability has been inferred from changes in the chemical concentrations of dust particles trapped in the peat (Kylander et al., 2005; Martínez Cortizas et al., 2002, 2007a; Shotyk, 1996; Shotyk et al. 2001;), and changes in vegetation cover and wet to dry transitions from geochemical compositions of mires (Kylander et al., 2013; Muller et al., 2008).

A complementary biogeochemical approach to mire studies focuses on the characterization of the peat organic matter, through the determination of isotopic signatures (δD, $\delta^{13}C$, $\delta^{15}N$, $\delta^{18}O$, $\delta^{34}S$) or its molecular composition (Buurman et al., 2006; Hong et al., 2001; Kaal et al., 2007; Loisel et al., 2010; Schellekens et al., 2011; Tillman et al., 2010;). The $\delta^{13}C$ has been applied on bulk peat or isolated compounds as a tool to explore the origin of the carbon (C_3, C_4 plants or aquatic origin) because photosynthesis fractionation signatures are commonly preserved (Meyers, 2003). Moreover, $\delta^{13}C$ together with δD and $\delta^{18}O$ can track hydrologic changes such as wet to dry transitions or changes in the precipitation-evaporation balance (Hong et al., 2001).

Stable isotopes can also be valuable indicators of organic matter origin and decay ($\delta^{13}C$, $\delta^{15}N$) (Aucour et al., 1999; Talbot and Johannessen, 1992), and redox changes ($\delta^{15}N$, $\delta^{34}S$) (Jędrysek and Skrzypek, 2005; Nóvak et al., 1999 and Talbot and Johannessen, 1992).

The majority of mire studies focus mainly on climate or environmental reconstructions using peat cores from ombrotrophic boreal and temperate mires of the Northern Hemisphere (Chambers and Charman, 2004; Clymo et al., 1984; Gorham and Janssens, 2005; Jackson and Charman, 2010; Shotyk, 1996). While receiving increasing attention during the last decades, peatlands in the Southern Hemisphere remain substantially less explored. Few studies have attempted to reconstruct environmental changes on tropical and subtropical mires (Dommain et al., 2011; Kylander et al., 2007; Muller et al., 2008; Page et al., 2010; Weiss et al., 2002). This study presents organic and inorganic biogeochemical data, including pollen analysis from the oldest Southern Hemisphere peat deposit studied to date (Easter Island), to track the environmental changes of the last ~70 kyr BP. While numerous studies have revealed the environmental changes on Easter Island using lacustrine sediments (Azizi and Flenley, 2008; Cañellas-Boltà et al.,2012; Cañellas-Boltà et al., 2013; Flenley and King, 1984; Flenley et al., 1991; Horrocks et al., 2012a, Horrocks et al., 2012b; Mann et al., 2008; Sáez et al., 2009), fewer works have been carried out on the Easter Island peat sequences. The Rano Aroi peat record has been analyzed using pollen (Flenley et al., 1991, Peteet et al., 2003) and XRF core scanner and stable isotope data (Margalef et al., 2013). Margalef et al. (2013) combined facies and macrofossil descriptions, bulk peat total carbon (TC), and total nitrogen (TN) and $\delta^{13}C$ data with XRF core scanner data (Ca, Fe and Ti elements) data to reconstruct environmental history of the site at a millennial time scale. However, to fully reveal the complex interactions and processes

126 controlling the geochemical signatures at Rano Aroi such as soil dust, flood events,
127 droughts and redox changes, more comprehensive geochemical analyses are needed.
128 Therefore, in this paper, we analyzed bulk peat samples to obtain absolute
129 concentrations of sixteen elements (Al, Fe, Ti, Ca, Mg, Sr, Y, Zr, Ba, Sc, V, Cr, Mn, Cu,
130 Cd, Th). This geochemical dataset is complemented with TC, TN, TS content and the
131 isotopic composition ($\delta^{13}C$, $\delta^{15}N$, $\delta^{34}S$) of the peat and pollen data. Only a few previous
132 studies are based on such a broad dataset including chemical and biological data from
133 the same peat record (Muller, 2006). This comprehensive approach combining inorganic
134 and organic geochemistry reinforced by pollen analysis allows us to establish links
135 between vegetation changes, mineral inputs and biogeochemical processes within peat
136 as a response to autogenic and external forcing. The results improve our understanding
137 of tropical and subtropical peat dynamics and the environmental and climatic history of
138 Easter Island since MIS 4 (~70 cal kyr BP).

139 **2. STUDY SITE**

140 Easter island (27º 07'S, 109º 22'W), known as Rapa Nui in the local language, is a
141 small volcanic island situated on the edge of South Pacific Convergence Zone (SPCZ),
142 Intertropical Convergence Zone (ITCZ) and South Pacific Anticyclone (SPA), the three
143 main features that determine the South Pacific climatic configuration (Fig. 1). The
144 climate is subtropical, with monthly average temperatures between 18 (August) and
145 24°C (February) and an extremely variable annual precipitation ranging from 500 to
146 1800 mm.

147 There are three permanent water bodies on the island, two lakes (Rano Raraku and
148 Rano Kao) and a mire (Rano Aroi) formed in a volcanic crater. The smooth slopes of the
149 inner part of the volcanic cone constitute the catchment (15.82 ha). The crater itself is
150 near the highest summit of the island, Mauna Terevaka (511 m a.s.l), composed by

highly porfiric olivinic tholeiite, hawaiite, and basaltic lava flows (Baker 1974, González-Ferran et al., 2004) and covered by andosols. The surface vegetation of the mire is characterized by *Scirpus californicus*, *Polygonum acuminatum*, *Asplenium polydon* var. *squamulosum*, *Vittaria elongata* and *Cyclosorus interruptus*, while the surrounding area is covered by grasslands and a small eucalyptus forest planted during the 1960s (Rull et al., 2010a). Rano Aroi is a minerotrophic fen, fed by rainfall and groundwater; hydrogeological and isotopic studies confirm that the system represents a perched spring connected to the main island aquifer (Herrera and Custodio, 2008; Margalef et al., 2013).

3. METHODOLOGY

In March 2006, a 14 m deep peat core (ARO 06 01) was collected in eleven sections from the central part of the mire with a UWITEC® corer, a modular percussion piston coring system. The first two meters of the sequence were not kept to avoid potential anthropic remobilization as described in the central part of the mire previously (Flenley and King, 1984; Flenley et al., 1991). The core sections were sealed, packed, transported to the laboratory and stored at 4 °C until sampling. Core sections were split longitudinally, imaged and the peat facies were described.

3.1 Geochemical analyses

On the core sections

The core was sampled every 5 cm for total carbon, nitrogen and sulphur (TC, TN, TS) and stable isotope ($\delta^{13}C$, $\delta^{15}N$, $\delta^{34}S$) analyses. The 218 samples were dried at 60°C over 48 hours, frozen with liquid nitrogen and ground in a ring mill. Total C, TN and their stable isotopes ($\delta^{13}C$ and $\delta^{15}N$) were analyzed using a Finnigan delta Plus EA-CF-IRMS spectrometer, and $\delta^{34}S$ measurements were performed using a Finnigan MAT CHN-IRMS Finnigan DeltaPlus XP (precision of 0.2‰ and 0.3‰ respectively). Both

instruments are located at the Serveis Cientifico-Tècnics (SCT) of the Universitat de Barcelona (UB).

To investigate the mineralogy and size of the mineral grains present in the levels with higher inorganic content (Margalef et al., 2013), three representative samples were selected; a level rich in Ca and Fe (4.8 m depth), and two silty levels with high values of Ti and Fe (8.3 and 10.55 m depth). These samples were dried and mineral grains were density separated in purified water. The grains were carefully attached to stubs using a conductive bioadhesive tape. A morphological description using a FEI ESEM-EDS in the *low vacuum mode* (around 0.5 torr) and *high vacuum mode* ($< 10^{-4}$ torr) was made on the selected samples in the SCT-UB. Stubs were carbon-coated before being observed in *high vacuum mode*. Secondary and backscattered electron images and Energy-dispersive X-ray spectroscopy (EDS) were used systematically to characterize the mineral grains.

All geochemical sample preparation for Inductively Coupled Plasma-Atomic Emission Spectrometry (ICP-AES) was performed under clean laboratory conditions using acid cleaned labware. Each 250 mg of sample was digested using a mixture of HNO_3/HBF_4 as described by Krachler et al. (2002). The microwave program included a 40 minute several-stage ramp to 200°C where samples were held for 20 minutes. The remaining solution was then transferred to Savillex vessels and evaporated on a hotplate at 50°C. Thereafter H_2O_2 was added and allowed to react for half a day. Samples were then sonicated and evaporated at 50°C. This was followed by a 2 day closed vessel digestion at 90°C with HNO_3. After sonication and evaporation at 50°C an additional cycle of H_2O_2 was made. Samples were once again evaporated and then taken up in 1% HNO_3 for analysis. The samples were analyzed for elemental concentrations using a Varian Vista AX ICP-AES at the Department of Geological Sciences, Stockholm

University, Sweden.

A suite of twenty elements were acquired including Al, Ba, Ca, Cd, Cr, Cu, K, Fe, Li, Mg, Mn, Na, Sc, Sr, Ti, Th, V, Y, Zn and Zr. To date, there is no certified reference material for peat that offers a wide range of elemental data. There is however a peat reference material NIMT/UOE/FM/001 that was tested and analyzed by Yafa et al. (2004). The analytical performance was thus assessed using this material as well as NIST SRM-2711a Montana Soil and NIST SRM-2586 Trace Elements in Soil. Five procedural replicates were made of each reference material. For NIMT/UOE/FM/001, our peat reference material, most elemental recoveries were high, ranging from 99% to 119%. Cadmium however had even higher recoveries (128%) while low recoveries were recorded for Ti (63%). For the other two reference materials, both soils, recoveries were much lower. For NIST SRM-2586 recoveries range from 70-91% for Al, Ba, Ca, Mg, Sc, Sr and Y and 53-66% for Cd, C, Fe, Mn, V and Zn. Again Ti had exceptionally low recoveries (44%) while Th had concentrations double the recommended values. For NIST SRM 2711a recoveries ranged between 64-84% with the exception of Ti (42%) and Th again had concentrations double the recommended values. Replicates of the reference materials were generally within 20% or better of each other. Procedural blanks for were below 3% of the average sample concentrations for the majority of the elements. Slightly higher blanks were found for Al and Mn (<5%), Ba and Cr (<12%) and Zr (<32%).

While the original intention was to make a total digestion of the peat samples, the reference materials suggest that this may not be the case. Although the recoveries for the peat reference material are high, the recoveries for the reference soils are much lower. Nonetheless, in a paleoenvironmental context the relative changes of the elements can still reveal past changes. For this reason all elements, even those with lower (Ti, for

example) or higher recoveries (Th, for example) or potentially high blanks (Zr, for example) were included in our interpretation. Some elements were removed from the dataset because of low concentrations in the peat samples (Li and K), contamination during sampling (Zn) or because the concentrations were close to the analytical detection limits (Na). In the case of Th and Zr particularly, both elements present high communalities in the PCA, suggesting that their signals are not just analytical noise, and their behavior has a coherent paleoenvironmental significance.

Rock and soil analyses

Determination of the elemental composition of rocks and surface soil samples from Rano Aroi and Rano Raraku craters and other parts of the island was performed on 16 samples. All soil samples (5 samples, see supporting information) were obtained from the surroundings of Rano Raraku crater, while rock samples (11 samples, see supporting information) were collected around the Rano Aroi, Rano Raraku craters and other parts of the island. All samples were ground in a ring mill and dried at 60°C for 24 h. Each 0.1 g of sample was then digested using a mixture of 2.5 ml HNO_3+ 5 ml HF + 2.5 ml $HClO_4$ in Teflon tubes at 135°C for 12 h. Finally, 1 ml of HNO_3 and 5 ml of purified water were added to dilute the sample for analysis. The analyses were carried out with a high-resolution ICP-MS (HR-ICP-MS), Element XR Thermo Scientific located at the LabGEOTOP service of the Institute of Earth Sciences Jaume Almera-CSIC (Barcelona). Twenty-three elements were measured. Results are provided in the supporting information (Table 1).

3.2 Pollen analysis

A subset of 25 samples (3-4 g of wet peat) equally distributed along the record were extracted from Rano Aroi peat record and processed for pollen analysis using standard laboratory procedures by Rull et al. (2010b), which include sieving, digestions with

KOH, HCl and HF, and acetolysis. As an exotic marker, one spore tablet of *Lycopodium* (Batch. No. 177745, Lund University, Sweden) per gram was added to each sample before processing. The slides were mounted in silicone oil (not permanents) to be counted under optical microscope using x40 and x60 objectives mounted on a ZEISS® microscope with x10 ocular (ZEISS® Axioplan, ZEISS® Axiostar plus, ZEISS® Axio Scope A1and ZEISS® Axio Lab. A1).

Pollen counting was carried out until at least a total of 200 pollen grains, excluding spores and aquatic and semi-aquatic plants except for samples with very low pollen concentration. Fern spores are presented as a sum of all spore types. The pollen results are presented in percentages excluding spores and aquatic plants. Spores and aquatic plants are represented as a percentage respect the pollen sum. The pollen zonation was performed using psimpoll 4.26 (Bennett, 2002) by optimal splitting (Bennett, 1996). The counting of pollen grains and spores was carried out by comparisons with reference books and atlases for pollen as Hesse et al. (2009); Heusser (1971); Hoeve and Hendriskse 1998; Tryon and Lugardon (1991); Reille (1992); and the online pollen and spore atlas APSA (2007).

Many questions about former flora ecology and distribution of Easter Island remain unsolved, despite that several works have tried to reconstruct vegetation changes from pollen analyses on lake sediments (Azizi and Flenley, 2008; Butler et al., 2004; Dumont et al., 1998; Cañellas-Boltà et al., 2013; Flenley and King, 1984; Flenley et al., 1991; Gossen, 2007) or from macrofossil remains on lacustrine records or archeological sites (Cañellas-Boltà et al., 2012; Dumont et al., 1998; Mann et al., 2008; Orliac and Orliac, 1998; Orliac, 2000; Peteet et al., 2003). As an important number of flora species are now extinct from the island and the native Easter Island flora has been intensely perturbed (Dubois et al., 2013; Rull et al., 2010a), it is not possible to reconstruct

paleoenvironments from pollen analyses using local modern analogues. For this reason, a comparison with other islands (Juan Fernández, Hawaii, Rapa Iti) is useful in order to reconstruct vegetation changes observed in the pollen analysis (see section 4.4 for more information).

3.3 Age-depth model

An age model was built from 19 radiocarbon AMS dates measured from pollen concentrates in the Poznan Radiocarbon Laboratory (Poland) (see Margalef et al., 2013 for full details). Pollen enrichment process followed a classical treatment (Faegri & Iversen, 1989; Moore et al., 1991) modified by Rull et al. (2010b). The AMS ages were calibrated using CALIB 6.02 software, and the INTCAL 98 curve (Reimer et al., 2004) and CalPal (Danzeglocke, 2008) for samples older than 20,000 radiocarbon yr BP. The age model was built by simple linear interpolation between the radiocarbon dates as described in Margalef et al. (2013).

3.4 Statistical analysis

Principal component analysis (PCA) was applied in order to reduce the large ICP-AES dataset to a smaller number of variables. These principal components (PC) could then be interpreted in terms of geochemical and environmental processes. SPSS version 22 statistical software was used to perform the PCA including varimax rotation over the previously logged (ln) and standardized ICP-AES dataset (Al, Ba, Ca, Cd, Cr, Cu, Fe, Mg, Mn, Sc, Sr, Ti, V, Y and Zr).

Correlation coefficients between stable isotopes, organic matter elemental composition and principal components scores were then calculated. To complement the integrative study of all proxies, multiple regression models (stepwise regression mode) using the scores of the extracted principal components (PCR analysis) were obtained for TC, TN, TS, $\delta^{13}C$, $\delta^{15}N$, $\delta^{34}S$ using SPSS version 22 software.

4. RESULTS

4.1 Peat facies and age model

The Rano Aroi core (ARO 06 01) is made up of radicel peat as defined by Succow and Joosten, (2001), consisting of fine roots (diameter < 1mm) with <10% comprising larger remains, from Cyperaceae, Poaceae and Polygonaceae (Margalef et al., 2013). Based on plant type and remain size, geochemistry and degree of peat decomposition, 4 peat facies have been defined (Margalef et al. 2013). **Facies A** (reddish peat) consists of coarse plant remains, with very high C/N (43-111) ratios and $\delta^{13}C$ values between -21‰ and -26‰. **Facies B** (granulated muddy peat) is a light brown peat with low mineral content, made up of coarse to mid-sized organic fragments, mostly roots and rootlets. This facies is characterized by high C/N (41-85) ratios and $\delta^{13}C$ values ranging from -14‰ to -26‰. **Facies C** (organic mud) is found as centimeter thick layers interbedding Facies B. These layers have high mineral contents, high TN (1.08-1.76%) and relatively light $\delta^{13}C$ values (-14‰ to -22‰). **Facies D** consists of dark and fine-grained peat and is highly decomposed (pictures of the described facies can be found in Margalef et al., 2013).

The age model revealed large changes in peat accumulation rates and the occurrence of a long hiatus in the sequence (see supporting information, Table 2). (1) The bottommost part of the sequence (8.75 m -13.9 m) was accumulated prior to 55 kyr BP and, in consequence, it is beyond the limits of radiocarbon dating. Because the accumulation rate between 55 and circa 40 cal kyr BP (3.7–8.72 m) is almost constant and the peat facies are the same until the base of the sequence, we make the initial assumption that accumulation rates were also relatively constant for the bottommost part of the sequence. Consequently, this part of the sequence has been dated by extrapolation using the accumulation rate of the upper section (3.7–8.72 m) of the core

sequence (see Margalef et al., 2013 for further details). (2) A sharp unconformity occurs at 4.25 m (39 cal kyr BP), where highly oxidized peat (Facies D) is overlaid by much less decomposed peat (Facies A). Dating results, the peat facies D and the biogeochemistry data suggest that during a certain period of time after 39 kyr cal BP the wetland underwent a long-term drought (with likely associated peat decomposition and loss) resulting in a subaerial exposure (Margalef et al., 2013). (3) Above the clear unconformity, our age model shows extraordinary low peat accumulation rates, and 16,000 years are represented by 104 cm (between 3.27 m and 4.31 m, see table 2 from supporting information).

4.2 Geochemistry on peat cores

4.2.1 Organic geochemistry

Total C concentrations are highly variable but without any specific trend, ranging from 40% to 70% (Fig. 2). $\delta^{13}C$ shows constant values around -14 ‰ between 14 m and 9 m shifting gradually to values around -26‰ from 9 m to 6 m, and staying around these more negative values for the uppermost five meters of the sequence. In addition to the long-term trend, the $\delta^{13}C$ curve also shows high-frequency changes (dips) and significantly lower values for Facies C between 11 m and 6 m (Fig 2 and 6; Margalef et al., 2013). Total N contents range between +0.5% and +1.75%. C/N ratios are between 33 and 111. $\delta^{15}N$ values oscillate between -2.03 and +8.87‰. Peat sections with the heaviest isotopic composition, above +8‰, are found at 12.4 m and 10.7 m depth and above 6 ‰ at 3.40 m depth (Fig. 2).

Total S values are low (less than 1%) and show a decreasing trend from the bottom of the core to 6 m depth, followed by a slight increase from this depth to the top of the core. On the other hand, the $\delta^{34}S$ record can be divided into two main sections: below 8 m the average value is +18.04 ± 0.88 ‰ and above this depth it is +19.33 ± 1.60‰. The

shift between the two sections occurs at 7.7-7.2 m. (Fig. 2).

4.2.1 Mineral grain found on peat cores geochemistry

Most of the mineral grains observed under electronic microscope showed evidence of transport or advanced weathering. At 8.3 m and 10.55 m depth small grains (30-500 μm) were rutile, ilmenite and quartz, while the bigger grains (≥500 μm) were composed of inosilicates (pyroxenes), plagioclases and quartz. The sample from 4.8 m depth showed smaller grains (10-20 μm) composed of iron, magnesium and aluminum oxides, quartz and organic compounds bound to Ca, Br and Mg. Some of these organic compounds were large up to 200 μm.

4.3 Rock and soil analyses

The elemental composition of selected rock and soil samples from the Rano Aroi watershed and other areas of the island was analyzed to investigate the origin of the inorganic fraction arriving to the mire. The ICP-MS analyses show that basalt, hawaiite and tholeiite rocks are especially rich in Fe_2O_3 (16-22%) and TiO (2.5-4.4%) (see supporting information Table 1) as documented by previous petrographic studies (Baker et al., 1974). The other major components are found in the following concentrations: Al_2O_3: 16-22%, MnO: 0.3-0.5 % and CaO: 3.3-9%. Minor and trace elements showed the following ranges: Sc: 24-39 μg g^{-1}, V: 170-500 μg g^{-1}, Co: 40-163 μg g^{-1}, Cr: 1-60 μg g^{-1}, Ni: 2.2-29.5 μg g^{-1}, Cu: 16-112 μg g^{-1}, Zn: 110-185 μg g^{-1}, Sr: 76-280 μg g^{-1}, Y: 40-85 μg g^{-1}, Zr: 276-497 μg g^{-1}, Ba: 107-202 μg g^{-1}, Th: 2.4-5.2 μg g^{-1} (Table 1 of supporting information). The rock samples around Rano Aroi are particularly enriched in Ti, Al, Sc, V, Cr, Ni, Cu and depleted in Y, Zr, and Ba, when compared to samples from other areas of the island. On the other hand, the Easter Island andosols sampled for this study were especially enriched in Al, Cr, Y, Zr and depleted in Mg, Ca, Sc, V, Co, Ni, Cu, Zn, and Sr compared to rock samples.

4.4 Peat ICP-AES data and PCA

A PCA was performed using the suite of selected elements from the bulk peat analysis. Three components explaining 85% of the matrix variance were identified. The absolute concentration variations for elements representative of these PCs are shown in Fig. 2. The results of the PCA are presented in terms of the factor loading of each element in the extracted PCs by showing the fractionation of the communalities (i.e., the proportion of the variation of each variable explained by each PC) (Fig. 3) and by the depth records of the PCs factor scores (Fig. 4). The first component (PC1, 40.8% of the variance) is tied mainly to V, Al, Sc, Cr, Cd and Y (with positive loadings between 0.71 and 0.93, Al shown in Fig. 2) and to a lesser extent to Ti, Zr, Cu and Mn (Ti and Zr shown in Fig. 2, communalities shown in Fig. 3). The second component (PC2, 23.1% of the variance) is characterized by large positive loadings (between 0.69 and 0.93) of Th, Fe, Mn and Ba (Fe shown in Fig. 2) with significant contributions from Ti, Zr and Sr (Ti and Zr shown in Fig. 2, communalities shown in Fig. 3). And the third component (PC3, 21.3% of the variance) is characterized by large positive loadings (between 0.87 and 0.94) of Mg, Ca and Sr and moderate ones of Cu and Ba (Ca shown in Fig. 2, communalities shown in Fig. 3).

PC1 shows high scores in the older section of the peat record (>55.5 kyr BP; 9 m). A clear shift from higher to lower values is observed between 55.5 and 41.5 cal kyr BP (9-5.16 m), followed by a rapid increase until 31cal kyr BP (3.76 m) and stabilization thereafter (Fig. 4). PC2 variability shows a peaky pattern. From the bottom of the core to 6.1 m PC2 scores present peaks at 10.6 m, 10.01 m, 8.7 m and 7.73 m. From 6.1 m to 4.8 m values become high and quite stable, then start to decline gradually until 2.96 m (Fig. 4). Two prominent peaks occur in this last interval (4.8-2.96 m): at 4.05 m and at 3.45 m, the latter being the maximum of the entire record. At the upper

part of the sequence, from 2.96 m to 2.40 m PC2 shows a progressive increase. The PC3 scores do not show a clear trend at the bottom of the sequence. From 10.49 m to 8.15 m there is a clear declining trend, and a marked see-saw pattern until 5.79 m. Scores rapidly increase from 5.79 m to 5.41 m, defining a broad peak up to 4.25 m. From 4.25 m to 3.16 m PC3 scores decline irregularly, but a clear peak stands out in this interval at 3.86 m. The uppermost part of the sequence presents an increasing trend, (Fig. 4).

4.5 Pollen record

In this work, only the most abundant taxa: Poaceae, *Arecaceae* , Asteraceae, *Coprosma* and Cyperaceae pollen types together with fern spores sum have been used. The following taxons are included as "others": Triumfetta, Acalypha, Trema (Ulmaceae), Pinus, Macaranga, Sapinus, Plantago plus indeterminate and unknown pollen types.

Asteraceae (arbustive types) are present in Hawaii, Rapa and Juan Fernandez Island although nowadays these are not found on Easter Island, (Brown, 1935; Flenley et al., 1991, Zizka, 1991). In Hawaii these small trees form scarce-forested landscapes in between true forest and bare lava flows (Flenley, 1991). Native and endemic Poaceae are mainly present in meadows and open landscapes. Some biogeographical and ecological constraints of the known species are given in Table 3 of the supporting Information. Based on the endocarp of fossil seeds, an endemic species of Arecaceae tree has been proposed: *Paschalococos disperta* (Dransfield et al., 1984). This endemic species is extremely similar to *Jubaea chilensis* (Dransfield et al., 1984, Flenley et al., 1991*)* and is presented as an emblematic case of extinction. *Coprosma* is a genus of flowering plants (small trees) present on many Pacific sites (New Zealand, Hawaii, Borneo, Rapa, Juan Fernández). It is nowadays completely extinct from Easter Island but found in ancient lake and peat sediments (Flenley, 1991; Horrocks et al., 2013).

Cyperaceae is another abundant pollen type predominantly representing taxa found in moist and waterlogged parts of grassland meadows or peatlands (supporting information, Table 3). Finally, fern spores also constitute an important part of Rano Aroi pollen record, in contrast to the low dominance of fern spores observed in Rano Raraku lake sediment cores (Cañellas-Boltà et al., 2013; Flenley et al., 1991).

Two significant zones were obtained (Fig.5) over the complete pollen dataset:

Zone I (13.9-7.48 m depth, 71-48.3 kyr BP) is characterized by the dominance of Poaceae (70-90%) with an important contribution of *Arecaceae*, *Coprosma* pollen and fern spores.

Zone II (7.48-2.35 m depth, 48.3-8.5 kyr BP) is defined by an increase of Asteraceae at the expense of Poaceae and Arecaceae pollen. The appearance of a higher amount of Cyperaceae, probably from the mire itself, is remarkable. The elevated number of fern spores indicates that these might have been growing in the vicinity of the mire. Cyperaceae as other aquatic and semiaquatic plants can be useful to determine local conditions because they grow specifically in moist and flooded areas. Because of the strong local signal they are not included in the sum to perform percentages.

This Zone has been divided in three subzones in the following manner:

-Zone IIa (7.48-5.8 m depth, 48.3-43 kyr BP): this subzone is characterized by very high percentages of Asteraceae pollen (up to 70.5% at 6.15 m depth) while Poaceae pollen percentage remains lower than in Zone I. Fern spores start to be more abundant, together with Cyperaceae that depict increasing percentages from bottom to top of the zone.

-Zone IIb: (5.8-3.4 m depth, 43-20.6 kyr BP). The subzone consists of a pollen assemblage with a lower percentage of Asteraceae and a higher contribution of Arecaceae , Cyperaceae and fern spores. This subzone also contains a hiatus at 4.25 m

451 (see section 4.1).

452 - Zone IIc (3.4-2.35 m depth, 20.6-8.5 kyr BP) is characterized by a considerable
453 reduction in Asteraceae and the dominance of Cyperaceae and ferns.

454 ***4.6 Correlation between inorganic and organic peat chemistry***

455 In the PCA described above we did not include the variables that characterize the
456 chemical nature of the organic matter, because our main objective was to determine the
457 chemical nature of the minerogenic fraction in the peat. The next step is to correlate the
458 first three PC with the chemical composition of the peat organic matter (TC, TN, TS,
459 and the isotopic composition) to look for covariance and to investigate the underlying
460 processes controlling the changes in peat inorganic and organic matter, and how
461 external and internal (i.e. postdepositional) processes have affected both the inorganic
462 and the organic chemistry. The largest correlation values (Table 1) were found between
463 PC1 scores and TN, C/N ratios, $\delta^{15}N$, $\delta^{13}C$ (r are 0.66, -0.62, 0.65 and 0.59
464 respectively). Lower, but significant correlations ($p<0.01$) were found between PC1 and
465 TS ($r = -0.45$), PC2 and $\delta^{13}C$ ($r = -0.31$), and PC3 and TC, C/N ratios and TS (r are 0.30,
466 0.32 and 0.35 respectively, Table 1).

467 This relatively weak correlation structure may indicate that peat organic chemistry
468 was mainly controlled by factors other than those governing the observed changes in the
469 inorganic chemistry. But it may also reflect that there was no single dominant control
470 and that all or a combination of factors is responsible for peat geochemistry. To check
471 the latter possibility we performed a multiple regression analysis using as input
472 variables the three extracted principal components. Such a multiple regression models is
473 called principal components regression, PCR (see for example Desta Fekedulegn et al.,
474 2002). The results of the PCR models can be found in Table 2. As expected, the models
475 show larger correlation coefficients. Nevertheless, TC and $\delta^{34}S$ show a low ($R = 0.35$

and R = 0.49, respectively) and TS only a moderate correlation (R = 0.66) with the principal components, which may be taken as evidence that C and S cycling in Rano Aroi was not only coupled to the main processes responsible for the changes in the inorganic chemistry. On the contrary, TN, C/N ratios, $\delta^{13}C$, and $\delta^{15}N$ show significantly larger correlation coefficients (R = 0.72-0.75). For these variables PC1 has the highest regression coefficients (positive for TN, $\delta^{13}C$, and $\delta^{15}N$, and negative for the C/N ratio; Table 2) and is thus the most influential. A visual representation of the adjustment of the predictive models to the original data can be found in the Figure 1 of the supporting information. For TN and C/N ratios the similarity of the records of observed and expected values are quite remarkable, while for $\delta^{13}C$ and $\delta^{15}N$ the model basically accounts for the long-term changes but not for the short term events. For TS the fitting between real and expected values is pretty good except for the section comprised between 6.34 and 5.54.

5. DISCUSSION

5.1 Factors controlling peat elemental composition

The PCA performed on the Rano Aroi inorganic elemental dataset identified three main components that enable an identification of specific variables for each component (i.e., chemical elements in this case) whose behavior is similar and, thereby, likely controlled by the same process (Reimann et al., 2008).

5.1.1. Long-term mineral fluxes of very fine particles

PC1 is characterized by large positive loadings (>0.7) of typically lithogenic elements (V, Al, Sc, Y, Ti, Zr*)* and some metals (Cr, Cd, Cu). These elements are associated with very fine particulate material and this component can confidently be related to the deposition of soil dust transported by wind together with contributions from hydric erosion. Given the isolation of Easter Island, this signal would be mainly

501 dominated by fluxes from the volcanic rocks and soils of the island itself. Elements on
502 this first component (like Al, Ti, Zr, Cr, Cu and other metals) are enriched in volcanic
503 soils with increasing degree of pedogenesis (Martínez Cortizas et al., 2007a). Almost
504 the same association of chemical elements (V, Al, Ti, Sc, Cu) was found by Muller et al.
505 (2008) in the study of the composition of the Lynch's Crater, a mire in NE Australia
506 with remarkable similarities with Rano Aroi (both mires are minerotrophic and formed
507 within a volcanic crater). The weathering of volcanic materials leads to the distribution of
508 this association of elements in (1) secondary minerals or organo-metallic compounds,
509 which are poorly crystalline or in (2) primary minerals, which are very resistant to
510 weathering. Most of these mineral phases are characterized by very fine (probably ≤ 50
511 μm) particles, which are easily mobilized by eolian or hydric erosion. This is consistent
512 with what is found after SEM observations on the Rano Aroi record because particle
513 size (except for Facies C) was dominated by fine silt and clay fractions (<30 μm).
514 Therefore, PC1 would track the long-term *background* fluxes of inorganic particulate
515 material coupled to soil pedogenesis and erosion (and factors affecting both). Fine
516 airborne dust particles are enriched in many elements compared to coarser ones
517 (Schuetz, 1989), and these chemical processes lead to potential physical and chemical
518 fractionation during dust transport, which seems to be more intense at short distances
519 from the source area and attenuates during long-range transport, as the grain size of the
520 dust decreases and homogenizes. The elemental composition reflected by PC1 is
521 consistent with these chemical enrichment processes associated to dust input variability.
522 *5.1.2 Strong runoff events and coarser detrital input*
523 The second component, PC2, is characterized by large positive loadings of Fe, Mn
524 and Ba and moderate positive loadings of Ti and Zr. These elements are associated to
525 coarser particles entering the mire. Non-systematic Scanning Electron Microscopy

526 (SEM) observations of the peat layers corresponding to high PC2 scores showed an
527 abundance of sand (50-600 μm) and coarse silt (20-50 μm) particles.

528 Iron and Mn are elements which can show a strong redox behavior, tending to be
529 depleted under anoxic conditions due to the mobility of their reduced forms and
530 accumulated under oxidizing conditions in peatlands (Chesworth et al., 2006;
531 Steinmann and Shotyk, 1997). Furthermore, PC2 variability (and the elemental profiles,
532 Figure 2) does not show a long-term trend as documented for redox sensitive elements
533 (i.e. Fe or Mn) in the Lynch's Crater record (Muller et al., 2008). However, the Rano
534 Aroi record has rather a peaky pattern resembling an "event signal". Despite its
535 potential mobility, Fe has been found to be immobile in certain peatlands (Muller et al.,
536 2008; Weiss et al., 2002) and previously formed Fe oxides/hydroxides were found to be
537 stable in lake sediments even under anoxic conditions (Gälman et al., 2009).
538 Additionally, in most soils developed on volcanic rocks such as those in the Rano Aroi
539 catchment, Fe is largely hosted by primary minerals and the Fe that is released during
540 weathering accumulates as non-crystalline or poor crystalline Fe forms (i.e. ferrihydrite,
541 Fe-organic matter associations) and secondary Fe phases (oxides and hydroxides)
542 (García-Rodeja et al., 2007). Barium, Ti, Th and Zr have only one oxidation state and
543 are not sensitive to redox changes, and major hosting minerals of Ba (barite, witherite),
544 Ti (ilmenite, rutile) and Zr (zircon, baddeyelite) are highly resistant to weathering. Thus,
545 in Rano Aroi PC2 is not likely to reflect diagenetic changes associated to changes in
546 redox conditions. Instead, while PC1 reflects the long-term particulate terrigenous input
547 into Rano Aroi, PC2 most likely represents strong, highly erosive runoff events capable
548 of transporting solid particles by suspension or eventually traction to the center of the
549 mire. Peaks in PC2 scores coincide with the presence of Facies C, organic mud, which
550 has been interpreted as being representative of wet events and higher water table levels

551 in the mire (Margalef et al., 2013).

552 *5.1.3 Post-depositional enrichments*

553 PC3 is characterized by large positive loadings of Ca, Sr, and Mg. These elements
554 are transported to the mire included in very fine soil particles (as primary minerals such
555 as plagioclase), but because they are also highly mobile as ions, they are transported to
556 the mire as dissolved species, too. Due to their chemical mobility, groundwater can also
557 greatly contribute to their distribution, sometimes by diffusion from the underlying
558 sediments as a result of the chemical dissolution of Ca-bearing minerals (Shotyk et al.,
559 2002). And, as essential nutrients, they are also subjected to intense biocycling.

560 The most prominent feature of the PC3 record is the maximum values (Fig. 4, Fig. 6,
561 Fig. 7) attained between ca. 42-39 kyr BP (4.25 m and 5.41 m depth) coinciding with
562 facies D (highly decomposed peat, Margalef et al., 2013). Age model, geochemistry and
563 the sharp discontinuity described at the uppermost limit of facies D suggest that there
564 was a loss (i.e. erosion) of previously accumulated peat layers. This would also mean
565 that the geochemical features exhibited below this sedimentary hiatus (between 5.41 m
566 and 4.25 m depth) were acquired thousand years later than accumulation, as diagenetic
567 changes caused by peat aereal exposure. Given this circumstance the most likely
568 explanation for enrichment on facies D was an intensive use of these elements as
569 bio nutrients by the plant community because a more intensive input of Ca, Mg and Sr
570 as a solute form would require a wetter climate. The lowering of the mire water table,
571 due to drought phases, is known to accelerate peat decomposition (Ise et al., 2008) and
572 produce an enrichment of certain elements in the peat (Biester et al., 2012; Martínez
573 Cortizas et al., 2007b). The increase of Ca –among other elements- at surface levels
574 when peat growth stagnates has been explained by Damman et al. (1992) as an effect of
575 the detritus cycle. At Lynch's Crater, Ca, Sr and Mg were also enriched in the more

decomposed peats (Muller et al. 2008). Another example of similar chemical enrichments comes from a Canadian mire composed of a 153-cm-thick layer of ombrotrophic, moderately decomposed peat overlying highly humified, minerotrophic peat: Ca was enriched 10 fold; Mg 2-3 fold; Fe (3 fold) in the highly decomposed peat (Zoltai and Johnson, 1985). In Rano Aroi the maximum concentrations for Ca, Mg and Sr in the c. 42-31 kyr BP (6-4 m depth) peat are around 5 fold, 3 fold and 2.5 fold higher than average concentrations in the peat deposited ca. 55-42 kyr BP (8-6 m).

5.2 Linking the organic and inorganic peat chemistry

5.2.1 PC1 and organic chemistry

The long-term variability of PC1 is similar to the long-term evolution of the $\delta^{13}C$ record from 55.5 to 43.9 kyr BP (9-6 m, Fig. 6) where both curves have a declining trend. The $\delta^{13}C$ trend shows a shift from values typical of C_4 plant types to lighter ones (characteristic of C_3 type) and suggests a change in the peat forming plant community (Margalef et al., 2013). This synchronicity between $\delta^{13}C$ and PC1 reveals an intimate relation between soil evolution and vegetation cover (see section 5.3).

The TN content decreases in the upper part of the sequence (Fig. 6) suggesting a link with soil evolution (PC1) and vegetation cover ($\delta^{13}C$). $\delta^{15}N$ (Fig. 2) can provide information on organic matter origin, nitrogen fixation ($\delta^{15}N$= 0 to +3 ‰) or plant productivity, but also syndepositional processes such as denitrification ($\delta^{15}N \geq +8$ ‰) (Handley et al., 1999; Meyers and Ishiwatari, 1993; Talbot and Johannessen, 1992). At Rano Aroi the average $\delta^{15}N$ is around +2.7 ‰, which is an isotopic signature typical of nitrogen fixation. The general $\delta^{15}N$ trend correlates directly with PC1 variation, as denoted by the high PCR regression coefficient (R= 0.56). Two hypotheses can be proposed to explain this relationship: (1) larger inputs of fine or very fine mineral particles to the mire may have triggered conditions of enhanced productivity and

601 consequently, higher $\delta^{15}N$ values; or (2) the vegetation change can entail a differential
602 fractionation of the peat forming plant remains (Talbot, 2001). However, two prominent
603 peaks of $\delta^{15}N$ at 66.8 kyr BP and 62.4 kyr BP (12.36 m and 11.07 m, Fig. 1 from
604 supporting information) are not accounted for by the PCR model and thus, they are
605 apparently not related to the influx of mineral matter or long term shifts (supporting
606 information, Fig. 1). These very high $\delta^{15}N$ values ($\delta^{15}N \geq 7$ ‰) may have been reached
607 by the preferential loss of light nitrogen through denitrification or ammonization (Talbot
608 et al., 2001) indicating anoxic phases. Therefore, our results suggest that different
609 processes could change the isotopic signature over different time scales: long-term
610 variability related to a shift in the vegetation and short-term variability related to small-
611 scale events such as a change in the potential redox.

612 Total S (decreasing) and $\delta^{34}S_{CDT}$ (increasing) trends from 55.5 to 43.9 kyr BP (9-6 m)
613 also show a differential S assimilation and fractionation through time (Fig. 2). The
614 changes in S cycling, especially $\delta^{34}S_{CDT}$, seem partially related to PC1 and the shift in
615 $\delta^{13}C$ (Table 1). Sulfur is incorporated by plants and bacteria, especially in the form of
616 organosulfur compounds, which seem to be the dominant S fraction in peat (Novák et
617 al., 1994 and 1999; Wieder and Lang, 1988). The chemical composition of the Rano
618 Aroi basin lithology indicates that inorganic S-content is low or negligible and this is
619 not considered a source of S to the mire (Baker et al., 1974, Margalef et al., 2013).
620 Because no volcanic eruption has been recorded nor have ash layers have been
621 described in Rano Aroi and Rano Raraku in late Quaternary sediments (Flenley 1991,
622 Sáez et al. 2009) the most likely dominant S source is marine sulphate. Variations in TS
623 and $\delta^{34}S_{CDT}$ can be therefore explained as changes in the loss after early diagenesis
624 (bacterial sulphate reduction and fixation) that discriminates against the heavier isotope
625 ^{34}S (see supporting information for additional information about sulphur interpretation).

626 *5.2.2 PC2 and organic chemistry*

627 PCR analyses show that organic matter composition does not significantly
628 correlate with PC2; however, several cause-effect relationships can be drawn from
629 the stable isotope, TC, and TN records. $\delta^{13}C$ second order changes (i.e. peaks) show
630 lower values coinciding with Facies C and PC2 peaks from the bottommost part of
631 the record until 6 m depth (Fig. 6). This relationship between organic matter and
632 Facies C can be explained by differential fractionation due to moisture changes or a
633 higher proportion of C_3 plants during wet events (Margalef et al., 2013). Abrupt
634 increases of TN also match PC2 peaks (Fig. 6). High TN values together with low
635 C/N ratios can be attributed to a higher contribution of lacustrine algal material
636 (low C/N), in contrast to high C/N values that indicate higher proportions of
637 terrestrial or aquatic plants (*versus* algae) organic matter (Meyers, 1994).

638 *5.2.3 PC3 and organic chemistry*

639 The organic chemistry does not correlate with PC3. Nevertheless, the drought event
640 may have partially determined the $\delta^{13}C$ signature like the lighter ratios on the highly
641 decomposed part of the record show. The same can be stated for the C/N ratios that are
642 slightly higher between 5 m and 4.23 m depth (Fig. 2). Total S displays a relative
643 enrichment between 5 m and 4.23 m depth while the underlying level, from 6.5 m to 5.5
644 m depth, becomes depleted in S. This pattern could respond to bioaccumulation through
645 the formation of organic S compounds that are more stable under oxidizing conditions
646 at the expense of the S released from the layers that remained under reducing conditions
647 near the watertable interphase (coherently when $\delta^{34}S_{CDT}$ reaches the maximum values).

648 ***5.3 Rano Aroi environmental reconstruction: climate, basin and peatland***
649 ***interactions***

650 The Rano Aroi dataset and our multi-proxy approach allow us to reconstruct

651 paleoenvironmental changes considering the intimate interplay between climate forcing,
652 basin and catchment evolution (soil and vegetation changes) and peat processes.

653 MIS 4 (73.5-59.4 kyr BP) is a period characterized by low southern Pacific SST
654 temperatures (Kaiser et al., 2005, Pena et al., 2008, Fig. 7H). The Antarctic Circumpolar
655 Current (ACC) was enhanced and the Southern Westerlies moved equatorward resulting
656 in sea ice export away from Antarctica (Kaiser et al., 2005). Sea level was globally low,
657 between 90 and 100 m below the present day (Grant et al., 2012, Fig. 7E), which has
658 been proposed as an important factor for Easter Island's hydrology and groundwater
659 levels as well as that of other small islands (Margalef et al., 2013). A lower sea level
660 would probably also cause lower groundwater levels. This time period sees a complete
661 dominance of C_4 plant types (mostly Poaceae) on the Rano Aroi basin and Terevaka
662 area (Fig. 6) and the presence of Arecaceae and *Coprosma* taxa on the island. Some
663 studies have proposed the development of palm tree forests preferentially in the lower
664 areas of the island (Flenley et al., 1991), although other authors suggest that the
665 palynological results obtained so far are also coherent with a mosaic vegetation pattern
666 with forested areas around permanent mires, lakes and the coastline as gallery forests
667 (Rull et al., 2010a).

668 The prevalence of C_4 plants suggests drier conditions that would lead to a low degree
669 of pedogenesis in the catchment soils; a scenario that is coherent with the low global
670 temperatures (Grant et al., 2012; Kaiser et al, 2005; Fig. 7H and E). Additionally,
671 herbaceous plant dominance may have facilitated higher soil erodibility, either eolian
672 and/or hydrological. The result was a higher dust flux of typical lithogenic elements and
673 metals into the mire, as summarized by PC1.

674 Globally warmer conditions heralded the arrival of MIS 3 (59.4-27.8 kyr BP). SST of
675 mid latitudes of Pacific Ocean increased around 5°C between 62.7 and 61.5 kyr BP

676 (Fig. 7H). This change was coupled to a rapid sea level rise, and between 62.9 and 61.2
677 kyr BP sea level shifted from -96 m a.s.l to -75 m a.s.l (Grant et al., 2012). In the South
678 Pacific, atmospheric patterns underwent important reorganizations. A record from the
679 Cariaco Basin (Peterson et al., 2000, Fig. 7F) indicates that between 61.2 and 59.9 kyr
680 BP the Intertropical Convergence Zone (ITCZ) was situated in a stable southern
681 position leading to very dry conditions in Northern Hemisphere tropics. The southern
682 latitudinal migration of ITCZ therefore leads to the opposite hydrologic trend for the
683 low latitudes in the Southern Hemisphere (Leduc et al., 2009; Wang et al., 2007,). The
684 early MIS3 has been characterized in the Rano Aroi record as a humid period, as
685 expressed by the abrupt events of higher sediment delivery (see section 5.1.2, and Fig. 6
686 and 7). It is significant that the first important wet event on Easter Island, starting in
687 Rano Aroi at 61.6 kyr BP is apparently synchronously with important global changes in
688 (1) sea level rise, (2) the position of the ITCZ and (3) SST.
689 The new warmer and wetter conditions of Early MIS 3 (61.6 to ~40 kyr cal BP) were
690 linked to an intensification of the degree of pedogenesis, which led to a decrease in the
691 flux of lithogenic elements to the mire. In parallel to the decline in PC1 values (Fig.
692 7B), the bulk peat stable isotope data values ($\delta^{13}C$ and $\delta^{15}N$) started a gradual decline at
693 55 cal kyr BP (Fig. 6). The isotopic change indicates a shift in the vegetation
694 community forming the peat, which becomes dominated by C_3 plant types. As stated in
695 previous sections, pollen data suggests that a complete dominance of Poaceae
696 (presumably C_4 species) was replaced by a combination of Asteraceae, *Coprosma*,
697 Poaceae and ferns between 51 and 48 kyr BP (Fig. 5). The vegetation change around the
698 mire and the presence of scarce forest, trees and shrubs may have prevented soil erosion
699 and reduced the fluxes of mineral matter to the mire (PC1). Finally, the expansion of
700 Cyperaceae (presumably C_3 species, such as *Scirpus californicus*) probably constituted

701 an important physical barrier during the C_3 dominance period, slowing the runoff input,
702 except during stronger events (PC2).
703 The late MIS 3 (40-27.8 cal. kyr BP) has been characterized as a drier phase on
704 Easter Island (Margalef et al., 2013). Sea level dropped relatively rapidly between 31.4
705 and 29.4 cal. kyr BP, but a South Pacific thermal response to global cooling was not
706 recorded until the onset of MIS 2 (Kaiser et al., 2005, Fig. 7H). The Cariaco Basin
707 record shows that between 35 and 31 cal. kyr BP, the ITCZ was in a northern position
708 preventing the arrival of strong storms to southern latitudes (Peterson et al., 2000, Fig.
709 7F). Moreover, several records from South America document intense dry between ca.
710 41 and ca. 31 cal. kyr BP (Lamy et al., 1998; Stuut and Lamy, 2004) explained by the
711 southern migration of the Southern Westerlies under the precession forcing (Fig. 7G).
712 The combination of these regional climate patterns likely led to a long dry period in the
713 Central Pacific and on Easter Island. The drought started after 39 cal. kyr BP, the age of
714 the sharp unconformity in the Rano Aroi sequence that separates highly degraded
715 (below) and fresh peat (above). A lowering of the Rano Aroi water table accelerated
716 peat decomposition producing an increase in the elements representative of PC3 (Ca, Sr,
717 and Mg) as a diagenetic imprint (Fig. 7D). The time interval above the discontinuity
718 depicts net accumulation rates of 0.05 mm/y (Fig. 7A) and represents the reactivation of
719 peat formation after a long-term pause (probably including erosion) where old carbon
720 could be incorporated in younger roots and plant remains. Because of this carbon
721 recycling, the chronology right after the reactivation has to be carefully considered and
722 the exact date of the reactivation and the amount of peat eroded cannot be properly
723 determined.
724 Although sea level reached a minimum ca. 23 cal. kyr BP (Grant et al., 2012;
725 Lambeck and Chappell, 2001; Fig. 7E) and could have negatively affected the

groundwater input and the hydrological balance at Rano Aroi, peat formation was active during the LGM. These can be explained by permanent cold conditions preventing strong evaporation (Sáez et al., 2009) and a northernmost position of Southern Westerlies whose influence reached subtropical latitudes during glacial times (Lamy et al., 1998, Fig. 7G).

Rano Aroi peat accumulation reactivated completely by ca. 17.5 kyr BP (the onset of Termination 1). Sea level started a prominent rise and the Intertropical Convergence Zone shifted to its furthermost south position between 21 and 16 kyr BP (Fig. 7F). During MIS 2 (27.8-14.7 cal. kyr BP), PC3 values remained low, showing no evidence of a drought period. Conversely, high PC2 events are found during the late glacial at 20.9-19.5 cal. kyr BP and 16.4 cal. kyr BP, likely representing enhanced precipitation coinciding with HS 2 and 1 (Fig. 7C). Maximum peat accumulation rates (14 cal kyr BP, Fig. 7A) coincide with the highest rates of sea level rise during deglaciation (Dickinson, 2001; Hanebuth et al., 2000; Lambeck and Chappell, 2001). Sea level rise together with warmer SST might have played an important role in the development of enhanced convection storms.

According to several Southern Hemisphere records the Early Holocene was characterized by a warming (Pena et al., 2008) and SST were maximal at approximately 12 cal kyr BP and generally decreased thereafter until modern SST were reached (Kaiser et al., 2005; Kaiser et al., 2008). In ARO 06 01 record, only the early Holocene (11.7-8.5 cal kyr BP) peat remains because the surface levels were rejected to avoid anthropic remobilization. The most important features characterizing this period are high PC2 values around 10.2 cal kyr BP indicating strong runoff events, while PC1 points to catchment soil conditions similar to those recorded ca. 48 kyr cal BP indicating relatively low fluxes of inorganic material under a permanent C_3 plant dominance (as

751 shown by $\delta^{13}C$, Fig. 6 and 7).

752 **6. CONCLUSIONS**

753 The organic matter composition (TC, TN, TS, $\delta^{13}C$, $\delta^{15}N$, $\delta^{34}S$), inorganic
754 geochemistry and pollen data from Rano Aroi mire provide a coherent reconstruction of
755 the paleoenvironmental history of Easter Island.

756 Principal components analysis of peat geochemistry reveals that three main
757 environmental processes have controlled the inorganic elemental composition of the
758 peat accumulated. (1) The first process, depicted by PC1, reflects changes in the basin
759 background erosion and transport of the mineral matter as very fine particles into the
760 mire and it is linked to soil evolution and vegetation shift. In Rano Aroi, $\delta^{13}C$ can be
761 used to infer an important vegetation change from C_4 to C_3 plant dominance that
762 occurred from 55 to 50 kyr BP. The correlation of the $\delta^{13}C$ and PC1 records reveals that
763 vegetation shifts and the evolution of the soils of the mire basin were intimately related
764 to the rate of allochtonous material transported into the peatland. These environmental
765 changes also affected the $\delta^{15}N$ signal that integrates variability in mire productivity and
766 redox conditions. $\delta^{34}S$ signatures indicate that the S source is primarily marine. The $\delta^{34}S$
767 ratio and TS concentration suggest that S may have been differentially mobilized
768 depending on vegetation assemblages by sulphate reduction bacteria. (2) The second
769 process is the occurrence of high precipitation events (identified by the PC2 signal)
770 related to strong runoff and delivery of large amounts of terrigenous particles coarser
771 than those mobilized by PC1 process. These events occurred at approximately 60 kyr
772 BP, 52 kyr cal BP and 42 kyr cal BP. (3) Finally, the third process, illustrated by PC3,
773 mainly reflects peat oxidation caused by a long-term drought after ca. 39 kyr cal BP.

774 The environmental evolution of Rano Aroi mire, largely driven by hydrological
775 changes, is coherent with the regional climatic variability described for the last 70 kyr

776 BP. During MIS 4 the Rano Aroi basin was occupied by open grasslands and C_4
777 Poaceae dominated the mire owing to the generally cold and relatively dry climate
778 conditions. MIS 3 was marked by the onset of wet events, which occurred at ca. 60 kyr
779 BP, 52 kyr cal BP and 42 kyr cal BP.

780 During the first half of MIS 3 and probably driven by the wetter and warmer
781 conditions, Asteraceae and other small trees became gradually more abundant, forming
782 scantily wooded areas around Terevaka, while C_3 peat forming plants colonized the Aroi
783 mire. In contrast, the second half of MIS 3 was drier. A long-term drought led to a water
784 table drop and enhanced peat mineralization at some time between the 39 and 31 kyr cal
785 BP. During the MIS 2 and LGM the water table recovered and peat accumulation
786 resumed under C_3 plant dominance.
787

AKNOWLEDGEMENTS

This research was funded by the Spanish Ministry of Science and Education through the projects LAVOLTER (CGL2004-00683/BTE), GEOBILA (CGL2007-60932/BTE) and CONSOLIDER GRACCIE (CSD2007-00067) and an undergraduate grant JAE (BOE 04/03/2008) to Olga Margalef. We would like to thank CONAF (Chile) and the Riroroko family for the facilities provided on Easter Island.

795 References

796 APSA Members* (2007) The Australasian Pollen and Spore Atlas V1.0. Australian
797 National University, Canberra. http://apsa.anu.edu.au/

798

799 Aucour, A. M., Bonnefille, R., Hillaire-Marcel, C., 1999. Sources and accumulation
800 rates of organic carbon in an equatorial peat bog (Burundi, East Africa) during the
801 Holocene: carbon isotope constraints. Palaeogeography, Palaeoclimatology,
802 Palaeoecology 150, 179–189.

803

804 Azizi, G., Flenley, J.R. 2008. The last glacial maximum climatic conditions on Easter
805 Island. Quaternary International 184, 166–176.

806

807 Baker, P.E., Buckley, F., Holland, J.G., 1974. Petrology and geochemistry of Easter
808 Island. Contributions to Mineralogy and Petrology 44, 85–100.

809

810 Barber, K.E., Chambers, F.M., Maddy, D., 2003. Holocene palaeoclimates from peat
811 stratigraphy: macrofossil proxy climate records from three oceanic raised bogs in
812 England and Ireland. Quaternary Science Reviews 22, 521–539.

813

814 Bennett K. D., 2002. Doucmentation for PSIMPOLL v. 4. 10 and PSCOMB V.1.03. c
815 programs for plotting pollen diagrams and analyzing pollen data.
816 http://www.chrono.qub.ac.uk/psimpoll/psimpoll.html/

817

818 Biester H, Hermanns Y-M, Martínez Cortizas A. 2012. The influence of organic
819 matter decay on the distribution of major and trace elements in ombrotrophic mires - a

820 case study from the Harz Mountains. Geochimica Cosmochimica Acta 84, 126-136.
821
822 Birks, H. H., Birks, H. J. B., 2006. Vegetation History and Archaeobotany 15, 235-
823 251.
824
825 Brown, F. B. H. 1935. Flora of Southeastern Polynesia, Vol. 3. Bernice P. Bishop
826 Museum Bulletin 130, 1-386.
827
828 Butler, K., Prior, C.A., Flenley, J.R., 2004. Anomalous radiocarbon dates from Easter
829 Island. Radiocarbon 46, 395–405.
830
831 Buurman, P., Nierop, K. G. J., Pontevedra-Pombal, X., & Martínez Cortizas, A.,
832 2006. Molecular chemistry by pyrolysis–GC/MS of selected samples of the Penido
833 Vello peat deposit, Galicia, NW Spain. Developments in Earth Surface Processes 9,
834 217-240.
835
836 Chambers F. M., Charman D. J., 2004. Holocene environmental change:
837 contributions from the peatland archive. The Holocene 14:1–6
838
839 Cañellas-Boltà N, Rull V, Sáez A, Margalef O, Bao R, Pla-Rabes S, Blaauw M,
840 Valero-Garcés B, Giralt S. 2013. Vegetation changes and human settlement of Easter
841 Island during the last millennia: a multiproxy study of the Lake Raraku sediments.
842 Quaternary Science Reviews 72, 36-48.
843
844 Cañellas-Boltá, N., Rull, V., Sáez, A., Margalef, O., Giralt, S., Pueyo, J.J., Birks,

H.H., Birks, H.J.B., Pla-Rabes, S., 2012. Macrofossils in Raraku Lake (Easter Island) integrated with sedimentary and geochemical records: towards a paleoecological synthesis. Quaternary Science Reviews 34, 113–126

Chesworth, W., Cortizas, A. M., & García-Rodeja, E.; 2006. The redox-pH approach to the geochemistry of the Earth's land surface, with application to peatlands. Developments in Earth surface processes, 9, 175-195.

Clement, A.C., Peterson, L.C.; 2008. Mechanisms of abrupt climate change of the last glacial period. Reviews of Geophysics 46 (4).

Clymo, R. S. 1984. The limits to peat bog growth. Philosophical Transactions of the Royal Society of London B 303, 605-654.

Damman A. W. H., Tolonen, K., Salanus, T., 1992. Element retention and removal in the ombrotrophic peat of Hadekeias, a boreal Finnish peat bog, Suo 43, 137-145.

Danzeglocke, U., Jöris, O., Weninger, B. 2008. CalPal-2007 online. http://www.calpal-online.de/ accessed 2009.05.03.

Desta Fekedulegn, B., JJ Colbert, RR Hicks, ME Schuckers. 2002. Coping with multicollinearity: an example on application of principal components regression in dendroecology. USDA Forest Service, Northeastern Research Station, Research Paper NE-721, 45 pp.

Dickinson, W.R., 2001. Paleoshoreline record of relative Holocene sea levels on Pacific islands. Earth-Science Reviews 55, 191–234.

Dommain, R., Couwenberg, J., Joosten, H., 2011. Development and carbon sequestration of tropical peat domes in south-east Asia: links to post-glacial sea-level changes and Holocene climate variability. Quaternary Science Reviews 30 (7–8), 999–1010.

Dransfield, J., Flenley, J.R., King, S.M., Harkness, D.D., Rapu, S., 1984. A recently extinct palm from Easter Island. Nature 312, 750–752.

Dubois, A., Lenne, P., Nahoe, E., Rauch, M., 2013. Plantas de Rapa Nui. Guía Ilustrada de la Flora de Interés Ecológico y Patrimonial. Umanga mo te Natura, CONAF, ONF International, Santiago, 132 pp.

Dumont, H.J., Cocquyt, C., Fontugne, M., Arnold, M., Reyss, J.-L., Bloemendal, J., Oldfield, F., Steenbergen, C.L.M., Korthals, H.J., Zeeb, B.A., 1998. The end of moai quarrying and its effect on Raraku Lake, Easter Island. Journal of Paleolimnology 20, 409–422

Faegri, K., Iversen, J., 1989. Textbook of Pollen Analysis, 4th Edition. Wiley, Chichester.

Flenley, J.R., King, S.M. 1984. Late Quaternary pollen records from Easter Island. Nature 307, 47–50.

Flenley, J.R., King, S.M., Jackson, J., Chew, C., Teller, J.T., Prentice, M.E., 1991. The Late Quaternary vegetational and climatic history of Easter Island. Journal of Quaternary Science 6 (2), 85-115.

Gälman V, Rydberg J, Shchukarev A, Sjöberg S, Martínez-Cortizas A, Bindler R, Renberg I. 2009. The role of iron and sulfur in the visual appearance of lake sediment varves. Journal of Pelolimnology 41, 141-153.

García-Rodeja E, Nóvoa JC, Pontevedra X, Martínez-Cortizas A, Buurman P. 2007. Aluminium and iron fractionation of European volcanic soils by selective dissolution techniques. In O Arnalds, F Bartoli, P Buurman, H Óskarsson, G Stoops, E García-Rodeja (eds) "Soils of volcanic regions in Europe", 326-351.

González-Ferran, O., Mazzuoli, R., Lahsen, A., 2004. In: Centro de Estudios Volcanológicos (Ed.), Geoloía del Complejo Volcánico Isla de Pascua Rapa Nui Santiago-Chile.1:30.000 Geol. map, (in Spanish).

Gorham, E., 1991. Northern peatlands: role in the carbon cycle and probable response to climatic warming. Ecological Applications 1, 182–195.

Gorham, E., Janssens, J.J., 2005. The distribution and accumulation of chemical elements in five peat cores from the mid-continent to the eastern coast of North America. Wetlands 25 (2) 259-278.

Gossen, C. 2007. Report: The mistery lies in the Scirpus. Rapa Nui Journal 21 (2), 105-110.

Grant, K. M., Rohling, E. J., Bar-Matthew, M. Ayalon, A. Medina-Elizalde, M., Bronk Ramsey, C., Satow, Roberts, A. P., 2012. Rapid coupling between ice volume and polar temperature over the past 150 kyr. Nature 491, 744–747

Handley L.L., Austin A.T., Robinson D., Scrimgeour C.M., Raven J.A., Heaton T.H.E., Schmidt S. and Stewart G.R., 1999. The 15N natural abundance ($\delta^{15}N$) of ecosystem samples reflects measures of water availability. Functional Plant Biology, 26(2), 185-199.

Hanebuth, T., Stattegger, K., Grootes, P.M., 2000. Rapid flooding of the Sunda Shelf: a late-glacial sea-level record. Science 288, 1033–1035.

Herrera, C., Custodio, E., 2008. Conceptual hydrogeological model of volcanic Easter Island (Chile) after chemical and isotopic surveys. Hydrogeology Journal 16 (7), 1329-1348.

Hesse, M., Halbritter, H., Zetter, R., Weber, M., Buchner, R., Frosch-Radivo, A., Ulrich, S., 2009. Pollen Terminology. An illustrated handbook. Springer WienNewYork. 261 pp

Heusser, C. J., 1971.Pollen and spores of chile: modern types of the pteridophyta, gymnospermae and angiospermae. The University of Arizona press. 165 pp.

Hoeve, M. L. and Hendrikse, M. (Eds.) 1998. A study of non-pollen objects in pollen slides the types as described by Dr. Bas van Geel and colleagues. Utrech.

Hong, Y. T, Jiang, H.B, Liu, T.S., Zhou, L.P., Beer, J., Li, H.D., Leng, X.T. Hong, B., Qin, X. G., 2001. Response of climate to solar forcing recorded in a 6000-year δ18O time series of Chinese peat cellulose, The Holocene 10, 1–7.

Horrocks, M., Baisden, W.T., Flenley, J., Feek, D., González Nualart, L., Haoa-Cardinali, S., Edmunds Gorman, T., 2012a. Fossil plant remains at Rano Raraku, Easter Island's statue quarry: evidence for past elevated lake level and ancient Polynesian agriculture. Journal of Paleolimnology 48 (4), 767-783.

Horrocks, M., Baisden, W.T., Nieuwoudt, M. K., Flenley, J., Feek, D., González Nualart, L., Haoa- Cardinali, S., Edmunds Gorman, T., 2012b. Microfossils of Polynesian cultigens in lake sediments cores from Rano Kau, Easter Island. Journal of Paleolimnology 47, Issue 2, pp 185-204.

Horrocks, M., Marra, M., Baisden, W. T., Flenley, J., Feek, D., Nualart, L. G., ... & Gorman, T. E., 2013. Pollen, phytoliths, arthropods and high-resolution ^{14}C sampling from Rano Kau, Easter Island: evidence for late Quaternary environments, ant (Formicidae) distributions and human activity. Journal of Paleolimnology, 1-16.

Ise T, Dunn AL, Wofsy SC, Moorcroft PR., 2008. High sensitivity of peat decomposition to climate change through water-table feedback. Nature Geoscience 1,

763-766.

Jackson, S.T., Charman, D. (Eds.), 2010. Editorial: “Peatlands: Paleoenvironments and carbon dynamics”. Peatlands: Palaeoenvironments and Carbon dynamics. Pages News 18.1 (2010): 3-4.

Jędrysek, Mariusz-Orion, and Grzegorz Skrzypek., 2005. Hydrogen, carbon and sulphur isotope ratios in peat: the role of diagenessis and water regimes in reconstruction of past climates. Environmental Chemistry Letters 2.4, 179-183.

Kaal, J., Baldock, J. A., Buurman, P., Nierop, K. G., Pontevedra-Pombal, X., & Martínez-Cortizas, A., 2007. Evaluating pyrolysis–GC/MS and ^{13} C CPMAS NMR in conjunction with a molecular mixing model of the Penido Vello peat deposit, NW Spain. Organic geochemistry 38 (7), 1097-1111.

Kaiser, J., Lamy, F., & Hebbeln, D., 2005. A 70‐kyr sea surface temperature record off southern Chile (Ocean Drilling Program Site 1233). Paleoceanography, 20 (4).

Krachler, M., Mohl, C., Emons, H., Shotyk, W., 2002. Influence of digestion procedures on the determination of rare earth elements in peat and plant samples by USN-ICP-MS. Journal of Analytical Atomic Spectrometry 17, 844-851.

Kylander, M. E., Weiss, D. J., Martínez Cortizas, A., Spiro, B., Garcia-Sanchez R., Coles, B. J. 2005 Refining the pre-industrial atmospheric Pb isotope evolution curve in Europe using an 8000 year old peat core from NW Spain. Earth and Planetary Science

995 Letters 240, 467-485.
996
997 Kylander, M.E., Muller, J., Wüst, R.A.J., Gallagher, K., Garcia-Sanchez, R., Coles,
998 B.J., Weiss, D.J., 2007. Rare earth element and Pb isotope variations in a 52 kyr peat
999 core from Lynch's Crater (NE Queensland, Australia): proxy development and
1000 application to paleoclimate in the Southern Hemisphere. Geochimica et Cosmochimica
1001 Acta 71, 942-960.
1002
1003 Kylander, M. E., Bindler, R., Martínez Cortizas, A., Gallagher, K., Mörth, C-M,
1004 Rauch, S., 2013. A novel geochemical approach to paleorecords of dust deposition and
1005 effective humidity: 8500 years of peat accumulation at Store Mosse (the "Great Bog"),
1006 Sweden. Quaternary Science Reviews 69, 69-82.
1007
1008 Lambeck, K., Chappell, J., 2001. Sea level change through the last glacial cycle.
1009 Science 292, 679–686.
1010
1011 Lamy, F., Hebbeln, D., Wefer, G. 1998. Late Quaternary precessional cycles of
1012 terrigenous sediment input off the Norte Chico, Chile (27.5S) and palaeoclimatic
1013 implications. Palaeogeography, Palaeoclimatology, Palaeoecology 141, 233-251.
1014
1015 Leduc, G., Vidal, L., Tachikawa, K., Bard, E. 2009. ITCZ rather than ENSO
1016 signature for abrupt climate changes across the tropical Pacific? Quaternary Research
1017 72, 123-131.
1018
1019 Loisel, J., Garneau, M., Hélie, J-F., 2010, Sphagnum $\delta^{13}C$ values as indicators of

palaeohydrological changes in a peat bot. The Holocene 20, 285-291.

Mann, D., Edwards, J., Chase, J., Beck, W., Reanier, R., Mass, M., Finney, B., Loret, J., 2008. Drought, vegetation change, and human history on Rapa Nui (Isla de Pascua, Easter Island). Quaternary Research 69, 16-28.

Margalef , O. Cañellas-Boltà, N., Pla-Rabes, S., Giralt, S., Pueyo, J. J., Joosten, H., Rull, V., Buchaca, T., Hernández, A., Valero-Garcés, B. L., Moreno, A., Sáez, A. 2013 A 70,000 year geochemical and palaeoecological record of climatic and environmental change from Rano Aroi peatland (Easter Island). Global and Planetary Change 108, 72-84.

Martínez Cortizas, A., García –Rodeja, E., Pontevedra Pombal, X., Nóvoa Muñoz, J. C., Weiss, D., Cheburkin, A., 2002. Atmospheric Pb deposition in Spain during the last 4600 years recorded by two ombrotrophic peat bogs and implications for the use of peat as archive. The Science of the Total Environtment 292, 33-34.

Martínez Cortizas A, Biester H, Mighall T, Bindler R. 2007a. Climate-driven enrichment of pollutants in peatlands. Biogeosciences 4, 905-911.

Martínez-Cortizas, A., Nóvoa, J. C., Pontevedra, X., Taboada, T., García-Rodeja, E., & Chesworth, W. 2007b. Elemental composition of reference European volcanic soils. In *Soils of Volcanic Regions in Europe* Springer Berlin Heidelberg, pp. 289-306.

Meyers P.A. and Ishiwatari R. 1993. Lacustrine organic geochemistry – an overview

of indicators of organic matter sources and diagenesis in lake sediments. Org. Geochem. 20: 867–900.

Meyers, P. A. 1994. Preservation of elemental and isotopic source identification of sedimentary organic matter. Chemical Geology 114, 289-302.

Meyers, P. A, 2003. Applications of organic geochemistry to paleolimnological reconstructions: a summary of examples from the Laurentian Great Lakes. Organic Geochemistry 34, 261-289.

Moore P.D.; Webb, J.A.; & Collinson, M.E., 1991. Pollen Analysis. Blackwell Scientific Publications.

Muller, J., 2006. Reconstructing climate change of the last 55 kyr: The Lynch's Crater peat mire record, NE-QLD, Australia. PhD thesis, James Cook University

Muller, J., Kylander, M.E., Wüst, R.A., Weiss, D.J., Martinez Cortizas, A., LeGrande, N., Jennerjahn, T., Behling, H., Anderson, W. T., Jacobson, G. 2008. Possible evidence for wet Heinrich phases in tropical NE Australia: the Lynch's Crater deposit. Quaternary Science Reviews, 27(5), 468-475.

Novák, M., Wieder, R. K., & Schell, W. R., 1994. Sulfur during early diagenesis in Sphagnum peat: Insights from $\delta^{34}S$ ratio profiles in ^{210}Pb-dated peat cores. Limnology and Oceanography, 39, 1172-1172.

Novák, M., Buzek, F., Adamová, M., 1999. Vertical trends in $\delta^{13}C$, $\delta^{15}N$, $\delta^{34}S$ ratios in bulk Sphagnum peat. Soil Biology and Biochemistry 31, 1343-1346.

Orliac, C. 2000. The woody vegetation of Easter Island between the early 14th and the mid-17th Centuries A.D. in Easter Island Archaeology: Research on Early Rapanui Culture, Stevenson, C., Ayres, W. (Eds.), Easter Island Foundation, Los Osos.

Orliac, C., Orliac, M., 1998. The disappearance of Easter Island's forest: overexploitation or climatic catastrophe? In Easter Island in Pacific Context: South Seas Symposium : Proceedings of the Fourth International Conference on Easter Island and East Polynesia., Stevenson, C., Lee, G., Morin, F.J. (Eds.) Easter Island Foundation, Los Osos, pp. 129–134.

Page, S., Wüst, R., Banks, C., 2010. Past and present carbon accumulation and loss in Southeast Asian peatlands. PAGES News, 18, 1, 25-26.

Pena, L. D., Cacho, I., Ferretti, P. and Hall, M. A. 2008. El Niño–Southern Oscillation–like variability during glacial terminations and interlatitudinal teleconnections, Paleoceanography, 23.

Peteet, D., Beck,W., Ortiz, J., O'Connell, S., Kurdyla, D., Mann, D., 2003. Rapid vegetational and sediment change from Rano Aroi crater, Easter Island. Easter Island. In: Loret, J., Tanacredi, J.T. (Eds.), Scientific exploration into the world's environmental problems in microcosm. Kluwer Academic/Plenum Publ., New York, pp. 81–92.

Peterson, L. C., Haug, G. H., Hughen, K. A., and Rohl, U., 2000. Rapid changes in the hydrologic cycle of the tropical Atlantic during the last glacial, Science 290, 1947–1951.

Reille, M., 1992. Pollen et spores d'Europe et d'Afrique du Nord. Laboratoire de Botanique historique et Palynologie. Marseille, 1992. 520 pp.

Reimer, P.J., Baillie, M.G.L, Bard, E., Bayliss, A., Beck, J.W., Bertrand, C.J.H, Blackwell, P.G., Buck, C.E., Burr, G.S., Cutler, K.B., Damon, P.E., Edwards, R.L., Fairbanks, R.G., Friedrich, M., Guilderson, T.P., Hogg, A.G., Hughen, K.A., Kromer, B., McCormac, G., Manning, S., Ramsey, C.B., Reimer, R.W., Remmele, S., Southon, J.R., Stuiver, M., Talamo, S., Taylor, F.W., van der Plicht, J., Weyhenmeyer, C.E., 2004. IntCal04 terrestrial radiocarbon age calibration, 0–26 cal kyr BP. Radiocarbon 46, 1029-1058

Reimann, C., Filzmoser, P., Garrett, R. G., & Dutter, R., 2008. Principal Component Analysis (PCA) and Factor Analysis (FA). *Statistical Data Analysis Explained: Applied Environmental Statistics with R*, 211-232.

Rull, V., Cañellas-Boltà, N., Sáez, A., Giralt, S., Pla, S., Margalef, O., 2010a. Paleoecology of Easter Island: evidence and uncertainties. Earth-Science Reviews 99, 50–60.

Rull, V., Stansell, N. D., Montoya, E., Bezada, M., and Abbott, M. B. 2010b Palynological signal of the Younger Dryas in tropical Venezuelan Andes. Quaternary

Science Reviews 29, 3045–3056

Sáez, A., Valero-Garcés, B., Giralt, S., Moreno, A., Bao, R., Pueyo, J.J., Hernández, A., Casas, D. 2009. Glacial to Holocene climate changes in the SE Pacific. The Raraku Lake sedimentary record (Easter Island, 27°S). Quaternary Science Reviews 28, 2743–2759.

Schellekens, J., & Buurman, P., 2011. *n*-Alkane distributions as palaeoclimatic proxies in ombrotrophic peat: The role of decomposition and dominant vegetation. Geoderma, *164* (3), 112-121.

Schuetz L., 1989. Atmospheric mineral dust - Properties and source markers in Paleoclimatology and Paleometeorology: Modern and Past Patterns of Global Atmospheric Transport, M. Leinen & M Sarthein (Eds) NATO ASI Series, Volume 282, 359-383.

Shotyk, W., 1996. Peat bog archives of atmospheric metal deposition: geochemical evaluation of peat profiles, natural variations in metal concentrations, and metal enrichment factors. Environmental Reviews, 4(2), 149-183.

Shotyk, W., Weiss, D., Kramers, J.D., Frei, R., Cheburkin, A.K., Gloor, M., Reese, S., 2001. Geochemistry of the peat bog at Etang de la Gruère, Jura Mountains, Switzerland, and its record of atmospheric Pb and lithogenic trace metals (Sc, Ti, Y, Zr, and REE) since 12,370 14C yr BP, Geochimica et Cosmochimica Acta, 65 2337– 2360.

1145 Shotyk W, Krachler M, Martínez-Cortizas A, Cheburkin A, Emons H., 2002. A peat
1146 bog record of natural, pre-anthropogenic enrichments of trace elements in atmospheric
1147 aerosols since 12370 ^{14}C yr BP, and their variation with Holocene climate change. Earth
1148 and Planetary Letters 199, 21-37.
1149
1150 Steinmann P, Shotyk W., 1997. Chemical composition, pH, redox state of sulfur and
1151 iron in complete vertical porewater profiles from two Sphagnum peat bogs, Jura
1152 Mountains, Switzerland. Geochimica Cosmochimica Acta 62, 1143-1163.
1153
1154 Stuut, J. B., Lamy, F., 2004. Climate variability at the southern boundaries of the
1155 Namib (southwestern Africa) and Atacama (northern Chile) coastal deserts during the
1156 last 120000 yr. Quaternary Research 62, 301-309.
1157
1158 Succow, M., Joosten, H. 2001. Landschaftsökologische Moorkunde. Stuttgart,
1159 Sweizerbart, 622 pp
1160
1161 Talbot, M.R., Johannessen, T., 1992. A high resolution palaeoclimatic record for the
1162 last 27,500 years in tropical West Africa from the carbon and nitrogen isotopic
1163 composition of lacustrine organic matter. Earth and Planetary Science Letters 110, 23–
1164 37.
1165
1166 Talbot, M.R. 2001, Nitrogen isotopes in palaeolimnology in: Tracking environmental
1167 change using lake sediments. Volume 2. Physical and geochemical methods, W.M. Last
1168 and J.P. Smol (Eds.), Kluwer Academic Press, Dordrecht , pp. 401-439.
1169

1170 Tillman, P. K., Holzkämper, S., Kuhry, P., Sannel, A. B. K., Loader, N. J., Robertson,
1171 I., 2010. Stable carbon and oxygen isotopes in Sphagnum fuscum peat from subarctic
1172 Canada: Implications for palaeoclimate studies. Chemical Geology 270, 216-226.
1173
1174 Tryon, A. F., Lugardon., 1991. Spores of the Pteridophyta. Springer-Verlag New
1175 York.
1176
1177 Wang, X., Auler, A. S., Edwards, R. L., Cheng, H., Ito, E., Wang, Y., Kong, X.,
1178 Solheid, M., 2007. Millennial-scale precipitation changes in southern Brazil over the
1179 past 90,000 years, Geophysical Research Letters, 34, 1-5.
1180
1181 Weiss, D., Shotyk, W., Rieley, J.O., Page, S.E., Gloor, M., Reese, S., Cortizas-
1182 Martínez, A., 2002. The geochemistry of major and selected trace elements in a forested
1183 peat bog, Kalimantan, SE Asia, and its implications for past atmospheric dust
1184 deposition. Geochimica et Cosmochimica Acta 66, 2307–2323.
1185
1186 Whitlock, C. and Larsen,C., 2001. Charcoal as afire proxy. In: Smol J.P., Birks,
1187 H.J.B. and Last, W.M. (Eds.), Tracking environmental change using lake sediments. Vol.
1188 3: Terrestrial, algal, and siliceous indicators. Kluwer, Dordrecht, pp. 75–98.
1189
1190 Wieder, R. K., & Lang, G. E., 1988. Cycling of inorganic and organic sulfur in peat
1191 from Big Run Bog, West Virginia. *Biogeochemistry*, *5*(2), 221-242.
1192
1193 Yafa C, Farmer JG, Bacon JR, Bindler R, Renberg I, Cheburkin A, Martinez Cortizas
1194 A, Dolgopolova A, Emons H, Krachler M, Shotyk W, Li XD, Norton SA, Pulford ID,

1195 Schweyer J, Kylander ME, Steinnes E, Weiss DJ, 2004. Development of a new
1196 ombrotrophic peat bog (low ash) reference material for the determination of elemental
1197 content. Journal of Environmental Monitoring 6:493-501.
1198
1199 Zizka, G., 1991. Flowering plants of Easer Island. Palmarum Hortus Francofurtensis
1200 Scientific Reports, 3, 1–108.
1201
1202 Zoltai SC, Johnson JD. 1985. Development of a treed bog island in a minerotrophic
1203 fen. Canadian Journal of Botany, 63, 1076-1085.
1204
1205

Table Caption

Table 1. Correlation coefficients between peat organic matter variables and the three Principal Components. In bold, significant correlation values at p-values > 0.01.

Table 2. Results of the multiple regression model (stepwise regression mode) using the scores of the extracted principal components obtained for TC, TN, TS, $\delta^{13}C$, $\delta^{15}N$, $\delta^{34}S$. R values indicates the multiple correlation coefficient analyses. The CP1, CP2 and CP3 columns indicate the regression coefficients derived from the PCR analysis.

Table

Click here to download Table: tables_def.docx

	N	PC1	PC2	PC3
TC	207	0.02	0.02	0.30
TN	207	**0.66**	0.10	-0.15
C/N	206	**-0.62**	-0.04	0.32
TS	194	**0.50**	-0.21	0.35
d13C	207	**0.59**	-0.31	0.29
d15N	207	**0.65**	0.11	0.15
d34S	194	-0.45	0.11	-0.02

Table 1.

	PC1	PC2	PC3	R
TC			0.330	0.35
TN	0.634	0.184	-0.184	**0.72**
C/N	-0.529		0.350	**0.75**
TS	0.453	-0.241	0.326	**0.66**
d13C	0.594	-0.302	0.306	**0.74**
d15N	0.560	0.140		**0.75**
d34S	-0.468			0.49

Table 2.

Figure captions

Figure 1. Situation of Eastern Island and main atmospheric patterns of Southern Pacific Ocean. Intertropical Convergence Zone (ICTZ) and South Pacific Convergence Zone (SPCZ) are form by the vertical motion of air masses and are associated to the cloud formation and the occurrence of thunderstorms. The Southern Westerlies (SW) are strong prevailing winds that blow eastward south from the subtropical highs, main drivers of extra tropical cyclones. Rano Aroi mire is a geogenous mire situated near the higher point of Easter Island (Terevaka summit).

Figure 2. Geochemical proxies analyzed over bulk peat in ARO 06 01 core versus depth. These are: TC, TN, TS (in percentages), C/N ratios, and $\delta^{13}C$, $\delta^{15}N$, $\delta^{34}S$ (‰) are indicative of the origin of organic matter and early diagnenetic processes. Elemental (Al, Ti, Zr, Fe, Ca) concentrations (in ppm) of the Rano Aroi peat deposits. Representative elemental profiles are shown for each of the factors. (Sc ans Zr for PC1, Fe and Zr for PC2, Sr for PC3).

Figure 3. Communalities of the elements. Light grey represents the element loadings related to the first component (PC 1), dark grey show the element loadings related to the second component (PC 2), black colour depicts the element loadings related to the third component (PC 3).

Figure 4. Variations of scores of PC1, PC2 and PC3 against depth in Rano Aroi peat sequence. PCA has been performed over ICP-AES dataset (Al, Ba, Ca, Cd, Cr, Cu, Fe, Mg, Mn, Sc, Sr, Ti, V, Y and Zr)

Figure 5. The more abundant pollen of Rano Aroi record are represented against depth: Poaceae, Palmae, Asteraceae, *Coprosma*, Fern sum, Cyperaceae and others. The results are presented as percentage over the pollen sum, excluding aquatic and semi-aquatic plants. Ferns and Cyperaceae percentage are presented over the pollen sum.

Figure 6. Synthesis of Rano Aroi environmental mire evolution. Stratigraphy and ages are shown. Four facies are distinguished in Rano Aroi: Facies A (Reddish peat), Facies B (granulated muddy peat), Facies C (organic mud) and Facies D (sapric peat). PC1 indicates changes in the long-term mineral matter fluxes (eolian and hydric) into the mire due to soil evolution and erosion. $\delta^{13}C$ shows an important vegetation change from C_4 to C_3 plant dominance occurred from 55 to 50 kyr BP. The $\delta^{13}C$ and PC1 record are directly related, evidencing the feedbacks between vegetation shifts and basin soil evolution. The occurrence of high precipitation events is showed by PC2 reflecting the input of large amounts of detrital material. PC3 tracks peat oxidation caused by a long term drought event.

Figure 7. Rano Aroi accumulation rates (A) and PC1, PC2 and PC3 scores obtained from the previous PCA analysis plotted against age together with a selection of environmental and climatic Southern Pacific records. Dotted line on Rano Aroi PC scores indicate the part of the record with chronological uncertainty (see text). From top to bottom: (B) PC1 scores suggest the transit from a period with elevate mineral input into the mire and C_4 plant type dominance to an scenario of C_3 dominance and lower mineral fluxes. (C) High values of PC2 scores might be interpreted as the occurrence of strong runoff events due to enhanced precipitation episodes. On the other hand, (D) high

PC3 scores suggest the mobilization of Sr, Ca, Mg due to peat exposure and oxidation. (E) Global sea level as indicator of the Easter island water table oscillations (Grant et al., 2012). (F) The reflectance record from Cariaco basin as indicative of changes in the latitudinal position of the ITCZ (Peterson et al., 2000). The southward migration of ITCZ has been related to higher precipitation rates over Southern tropical Pacific and intensification of SPCZ, bringing humid conditions to Easter Island. (G) Aridity index obtained by Stuut and Lamy (2004) using Chilean offshore coastal sediments to reconstruct the latitudinal position of Southern Westerlies (SW). A northern position of these prevailing winds contributes to transport the SPCZ cyclones to Easter Island. (H) Southern Pacific Sea Surface Temperatures at 41º latitude for the last 70 kyr BP (Kaiser et al., 2005).

Figure

Click here to download high resolution image

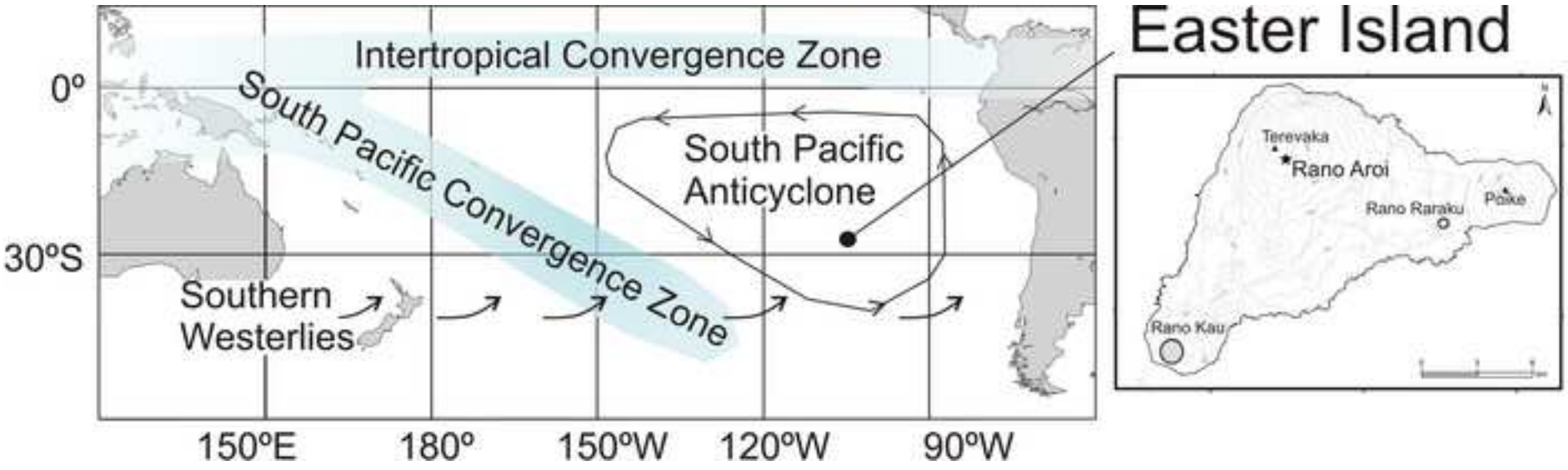

Figure

Click here to download high resolution image

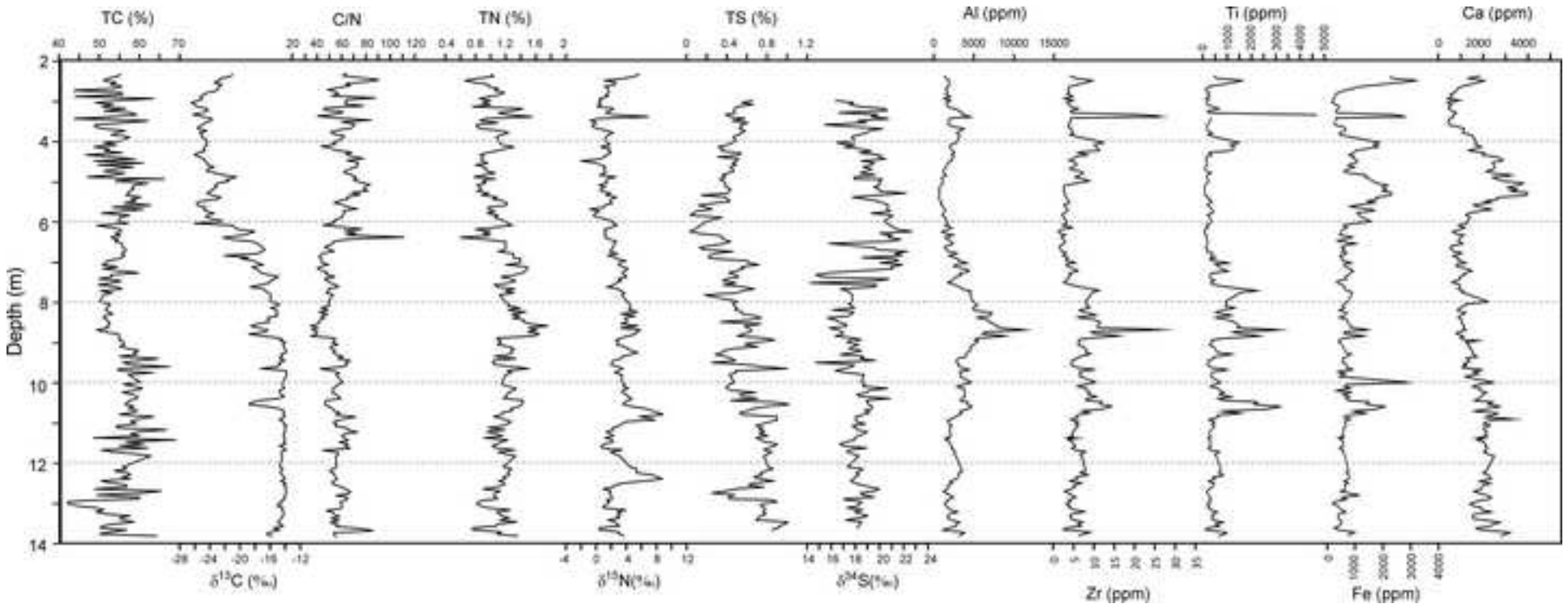

Figure
Click here to download high resolution image

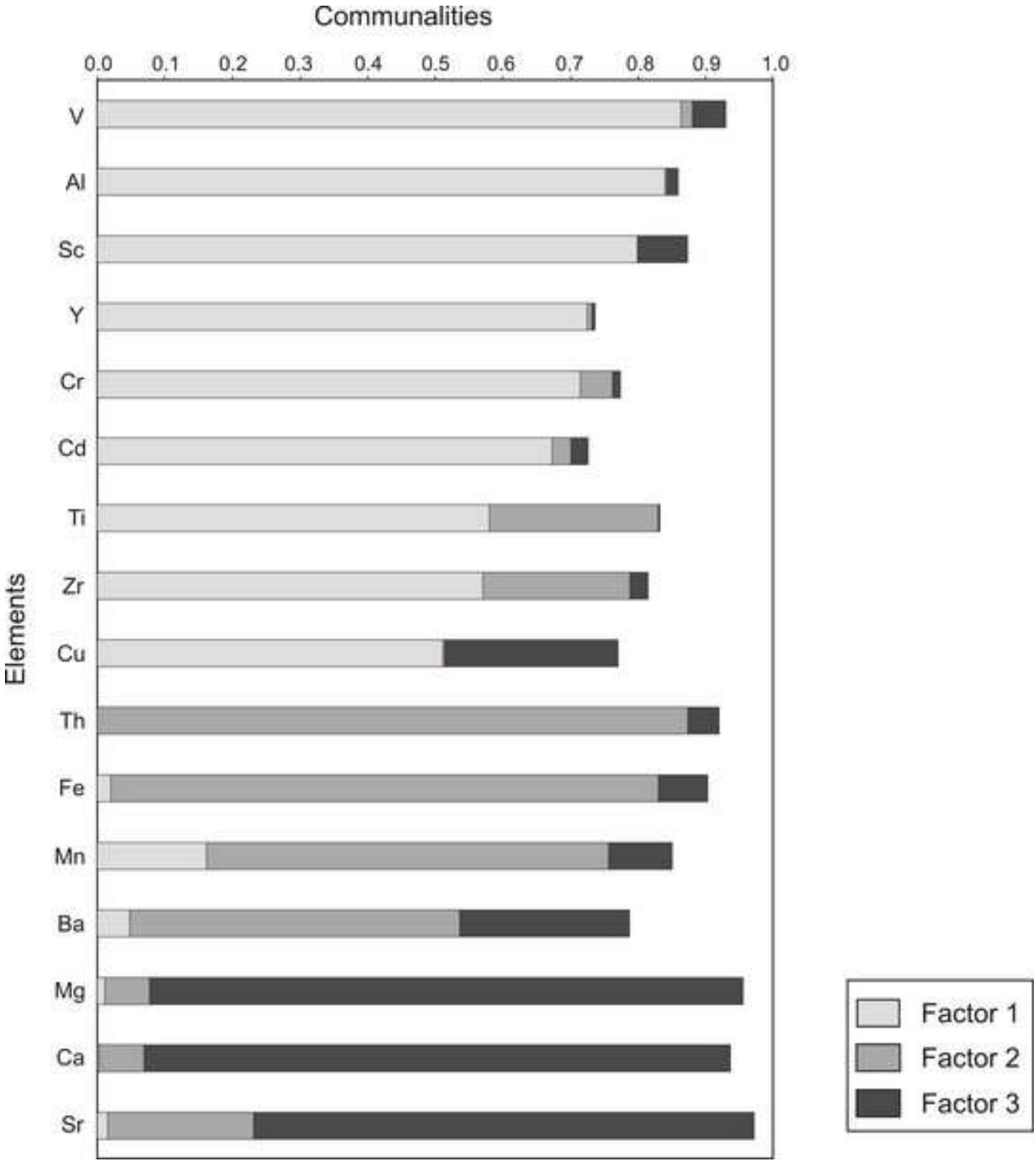

Figure

Click here to download high resolution image

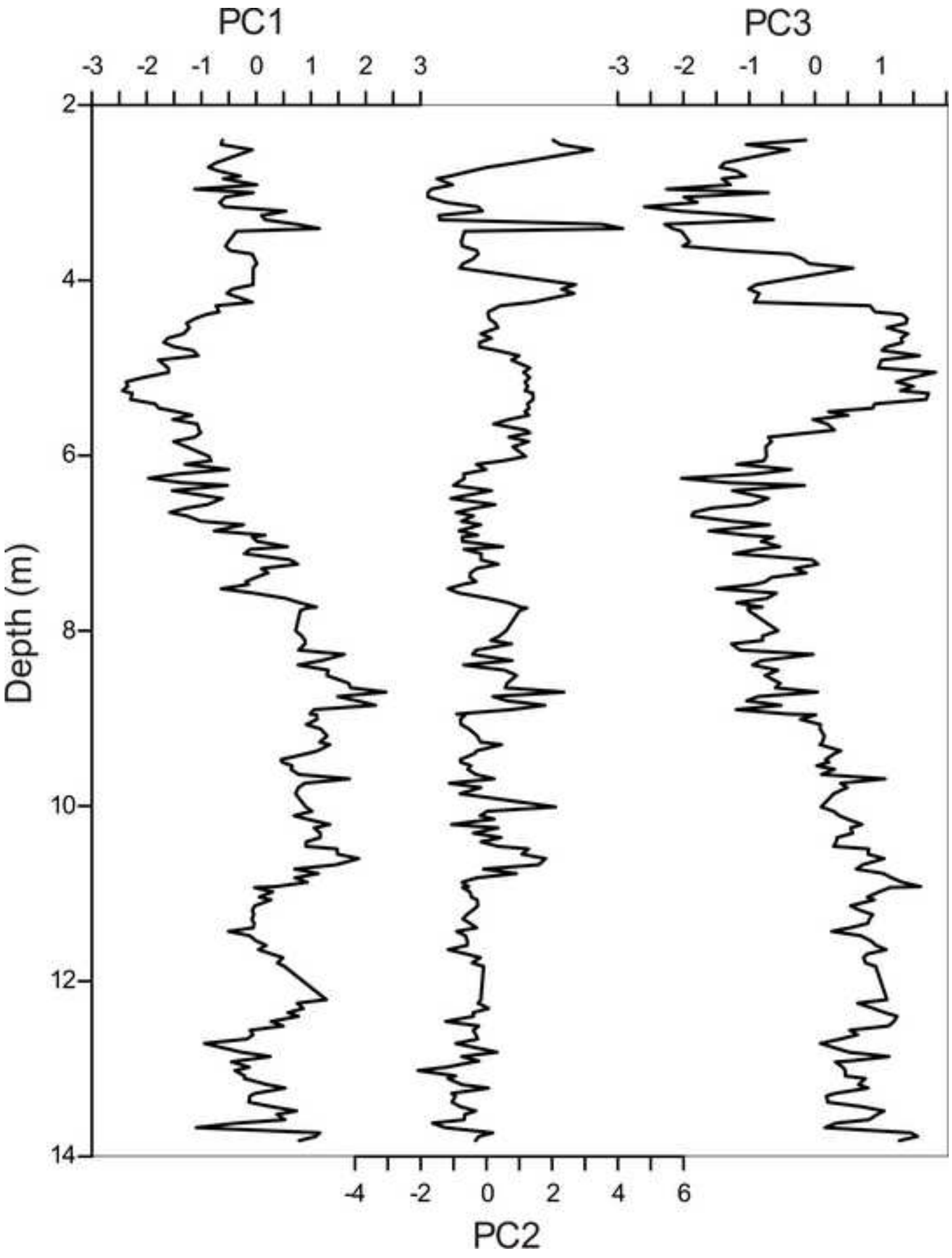

Figure

Click here to download high resolution image

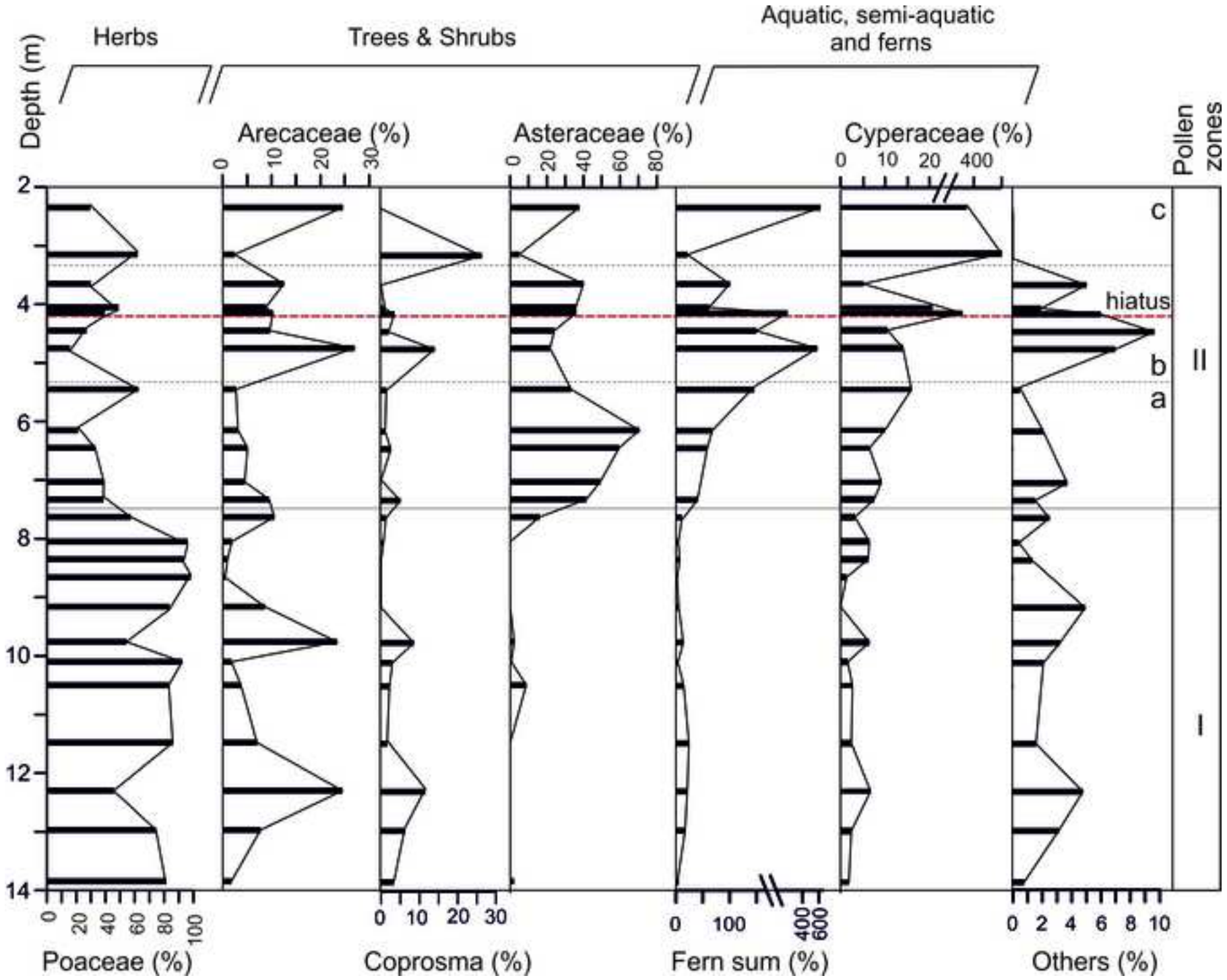

Figure

Click here to download high resolution image

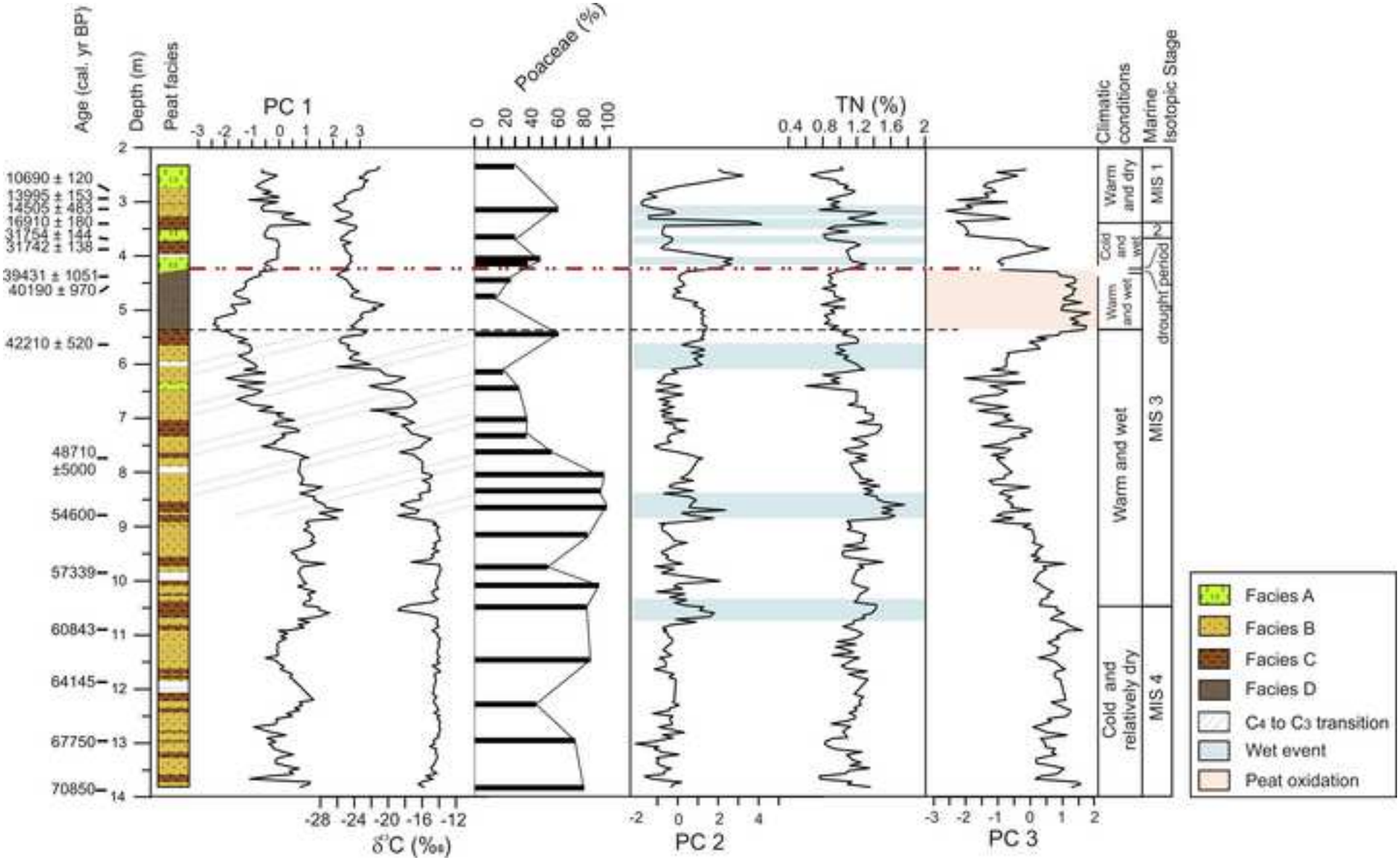

Figure

Click here to download high resolution image

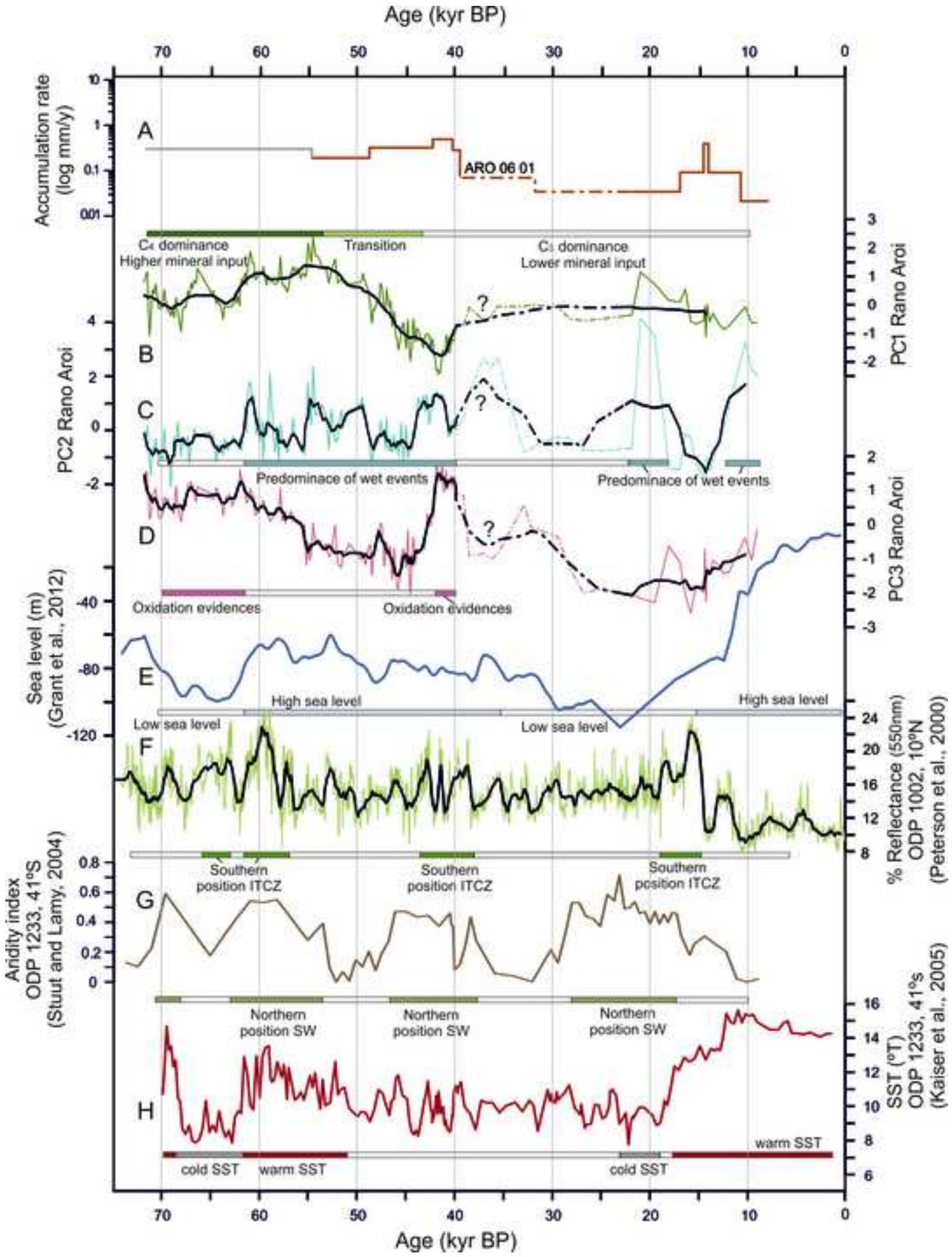

Background dataset for online publication only

Click here to download Background dataset for online publication only: Supporting information rv.docx

KML File (for GoogleMaps)

Click here to download KML File (for GoogleMaps): Rano Aroi.kml

Environmental processes in Rano Aroi (Easter Island) peat geochemistry forced by climate variability during the last 70 kyr

Margalef, O. [(1)], Martínez Cortizas, A. [(2)], Kylander, M. [(3)], Pla-Rabes, S. [(4,5)], Cañellas-Boltà, N.[(6,7)], Pueyo, J.J.[(7)], Sáez, A. [(7)], Valero-Garcés, B. L. [(8)], Giralt, S. [(1)]

[(1)] Institute of Earth Sciences Jaume Almera (ICTJA-CSIC), Sedimentary Geology and Geohazards, Lluís Solé i Sabarís s/n, E-08028 Barcelona, Spain (omargalefgeo@gmail.com)

[(2)] Departmento de Edafoloxía e Química Agrícola, Fac. de Bioloxía – Campus Vida, E-15782 Santiago, Spain

[(3)] Department of Geological Sciences and the Bolin Centre for Climate Research, Stockholm University, SE 10961 Stockholm, Sweden

[(4)] Ecological Research Center and Forestry Applications (CREAF). Campus de Bellaterra (UAB) 08193 Cerdanyola del Vallès, Barcelona. Spain.

[(5)] Advanced Studies Center of Blanes (CEAB-CSIC). C/ D'accés a la Cala St. Francesc, 14. Blanes. Girona. E-17300 Spain.

[(6)] Laboratory of Palynology and Paleoecology, Botanic Institute of Barcelona (IBB-CSIC-ICUB), Spain

[(7)] Faculty of Geology, Universitat de Barcelona, Martí i Franquès s/n, E-08028 Barcelona, Spain

[(8)] Instituto Pirenaico de Ecología (IPE-CSIC). Avda. de Montañana, 1005. 50059 Zaragoza, Spain

ABSTRACT

We analyze the geochemistry of Rano Aroi mire record (Easter Island) using bulk peat composition (C, N, S) and stable isotopes ($\delta^{13}C$, $\delta^{15}N$, $\delta^{34}S$) and major, minor and trace elemental composition obtained by ICP-AES (Al, Ti, Zr, Sc, V, Y, Fe, Mn, Th, Ba, Ca, Mg and Sr). Peat geochemistry and the pollen record are used to reconstruct the environmental changes during the last 70 kyr BP. Principal component analysis on ICP-AES data revealed that three main components account for the chemical signatures of the peat. The first component, characterized by lithogenic elements (combined signal of V, Al, Sc, Y, Cr, Cd, Ti, Zr and Cu), evidences long-term changes in the basal fluxes of mineral material into the mire. This component, in combination with stable isotopes and pollen data suggests a link between soil erosion and vegetation cover changes in the Rano Aroi watershed. The second component is identified by the signal of Fe, Mn, Th, Ba, Zr and Ti, and is indicative of strong runoff events during enhanced precipitation periods. The third component (tied mainly to Ca, Sr and Mg) reflects a strong peat oxidation event that occurred during an arid period with more frequent droughts, sometime between 39 and 31 kyr BP. Correlation coefficients and a multiple regression model (PCR analysis) between peat organic chemistry and the principal components of ICP-AES analysis were calculated. Isotope chemistry of the peat organic matter further contributes to define Rano Aroi environmental history: $\delta^{13}C$ data corroborates a vegetation shift documented by the palynological record from C_4 to C_3 between 55 and 45 kyr cal BP; the $\delta^{15}N$ record identifies periods of changes in mire productivity and denitrification processes, while the $\delta^{34}S$ peat signature indicates a marine origin of S and significant diagenetic cycling. The geochemical and environmental evolution of Rano Aroi mire is coherent with the regional climatic variability and suggests that climate was the main forcing in mire evolution during the last 70 kyr BP. The coupling

of geochemical and biological proxies improves our ability to decipher depositional processes in tropical and subtropical peatlands and to use these sequences for paleoenvironmental and paleoclimate reconstructions.

1. INTRODUCTION

Peatlands are paleoenvironmental archives capable of registering atmospheric, hydrological and ecological changes in the past (Jackson and Charman, 2010). Researchers have traditionally studied peat accumulation and decay dynamics (Clymo, 1984), and attempted to understand the contribution of these organic soils to the global carbon cycle (Gorham, 1991), as well as to reconstruct paleoecological changes using macrofossils, pollen (Barber et al., 2003; Birks and Birks, 2006) and charcoal remains (Whitlock and Larsen, 2001). In more recent times, inorganic geochemical proxies from peat sequences have increasingly been used to obtain high-resolution climatic and environmental reconstructions. For example, wind regime variability has been inferred from changes in the chemical concentrations of dust particles trapped in the peat (Kylander et al., 2005; Martínez Cortizas et al., 2002, 2007a; Shotyk, 1996; Shotyk et al. 2001;), and changes in vegetation cover and wet to dry transitions from geochemical compositions of mires (Kylander et al., 2013; Muller et al., 2008).

A complementary biogeochemical approach to mire studies focuses on the characterization of the peat organic matter, through the determination of isotopic signatures (δD, $\delta^{13}C$, $\delta^{15}N$, $\delta^{18}O$, $\delta^{34}S$) or its molecular composition (Buurman et al., 2006; Hong et al., 2001; Kaal et al., 2007; Loisel et al., 2010; Schellekens et al., 2011; Tillman et al., 2010;). The $\delta^{13}C$ has been applied on bulk peat or isolated compounds as a tool to explore the origin of the carbon (C_3, C_4 plants or aquatic origin) because photosynthesis fractionation signatures are commonly preserved (Meyers, 2003). Moreover, $\delta^{13}C$ together with δD and $\delta^{18}O$ can track hydrologic changes such as wet to dry transitions or changes in the precipitation-evaporation balance (Hong et al., 2001).

Stable isotopes can also be valuable indicators of organic matter origin and decay ($\delta^{13}C$, $\delta^{15}N$) (Aucour et al., 1999; Talbot and Johannessen, 1992), and redox changes ($\delta^{15}N$, $\delta^{34}S$) (Jędrysek and Skrzypek, 2005; Nóvak et al., 1999 and Talbot and Johannessen, 1992).

The majority of mire studies focus mainly on climate or environmental reconstructions using peat cores from ombrotrophic boreal and temperate mires of the Northern Hemisphere (Chambers and Charman, 2004; Clymo et al., 1984; Gorham and Janssens, 2005; Jackson and Charman, 2010; Shotyk, 1996). While receiving increasing attention during the last decades, peatlands in the Southern Hemisphere remain substantially less explored. Few studies have attempted to reconstruct environmental changes on tropical and subtropical mires (Dommain et al., 2011; Kylander et al., 2007; Muller et al., 2008; Page et al., 2010; Weiss et al., 2002). This study presents organic and inorganic biogeochemical data, including pollen analysis from the oldest Southern Hemisphere peat deposit studied to date (Easter Island), to track the environmental changes of the last ~70 kyr BP. While numerous studies have revealed the environmental changes on Easter Island using lacustrine sediments (Azizi and Flenley, 2008; Cañellas-Boltà et al.,2012; Cañellas-Boltà et al., 2013; Flenley and King, 1984; Flenley et al., 1991; Horrocks et al., 2012a, Horrocks et al., 2012b; Mann et al., 2008; Sáez et al., 2009), fewer works have been carried out on the Easter Island peat sequences. The Rano Aroi peat record has been analyzed using pollen (Flenley et al., 1991, Peteet et al., 2003) and XRF core scanner and stable isotope data (Margalef et al., 2013). Margalef et al. (2013) combined facies and macrofossil descriptions, bulk peat total carbon (TC), and total nitrogen (TN) and $\delta^{13}C$ data with XRF core scanner data (Ca, Fe and Ti elements) data to reconstruct environmental history of the site at a millennial time scale. However, to fully reveal the complex interactions and processes

126 controlling the geochemical signatures at Rano Aroi such as soil dust, flood events,
127 droughts and redox changes, more comprehensive geochemical analyses are needed.
128 Therefore, in this paper, we analyzed bulk peat samples to obtain absolute
129 concentrations of sixteen elements (Al, Fe, Ti, Ca, Mg, Sr, Y, Zr, Ba, Sc, V, Cr, Mn, Cu,
130 Cd, Th). This geochemical dataset is complemented with TC, TN, TS content and the
131 isotopic composition ($\delta^{13}C$, $\delta^{15}N$, $\delta^{34}S$) of the peat and pollen data. Only a few previous
132 studies are based on such a broad dataset including chemical and biological data from
133 the same peat record (Muller, 2006). This comprehensive approach combining inorganic
134 and organic geochemistry reinforced by pollen analysis allows us to establish links
135 between vegetation changes, mineral inputs and biogeochemical processes within peat
136 as a response to autogenic and external forcing. The results improve our understanding
137 of tropical and subtropical peat dynamics and the environmental and climatic history of
138 Easter Island since MIS 4 (~70 cal kyr BP).

139 **2. STUDY SITE**

140 Easter island (27º 07'S, 109º 22'W), known as Rapa Nui in the local language, is a
141 small volcanic island situated on the edge of South Pacific Convergence Zone (SPCZ),
142 Intertropical Convergence Zone (ITCZ) and South Pacific Anticyclone (SPA), the three
143 main features that determine the South Pacific climatic configuration (Fig. 1). The
144 climate is subtropical, with monthly average temperatures between 18 (August) and
145 24°C (February) and an extremely variable annual precipitation ranging from 500 to
146 1800 mm.

147 There are three permanent water bodies on the island, two lakes (Rano Raraku and
148 Rano Kao) and a mire (Rano Aroi) formed in a volcanic crater. The smooth slopes of the
149 inner part of the volcanic cone constitute the catchment (15.82 ha). The crater itself is
150 near the highest summit of the island, Mauna Terevaka (511 m a.s.l), composed by

highly porfiric olivinic tholeiite, hawaiite, and basaltic lava flows (Baker 1974, González-Ferran et al., 2004) and covered by andosols. The surface vegetation of the mire is characterized by *Scirpus californicus, Polygonum acuminatum, Asplenium polydon* var. *squamulosum, Vittaria elongata* and *Cyclosorus interruptus,* while the surrounding area is covered by grasslands and a small eucalyptus forest planted during the 1960s (Rull et al., 2010a). Rano Aroi is a minerotrophic fen, fed by rainfall and groundwater; hydrogeological and isotopic studies confirm that the system represents a perched spring connected to the main island aquifer (Herrera and Custodio, 2008; Margalef et al., 2013).

3. METHODOLOGY

In March 2006, a 14 m deep peat core (ARO 06 01) was collected in eleven sections from the central part of the mire with a UWITEC® corer, a modular percussion piston coring system. The first two meters of the sequence were not kept to avoid potential anthropic remobilization as described in the central part of the mire previously (Flenley and King, 1984; Flenley et al., 1991). The core sections were sealed, packed, transported to the laboratory and stored at 4 °C until sampling. Core sections were split longitudinally, imaged and the peat facies were described.

3.1 Geochemical analyses

On the core sections

The core was sampled every 5 cm for total carbon, nitrogen and sulphur (TC, TN, TS) and stable isotope ($\delta^{13}C$, $\delta^{15}N$, $\delta^{34}S$) analyses. The 218 samples were dried at 60°C over 48 hours, frozen with liquid nitrogen and ground in a ring mill. Total C, TN and their stable isotopes ($\delta^{13}C$ and $\delta^{15}N$) were analyzed using a Finnigan delta Plus EA-CF-IRMS spectrometer, and $\delta^{34}S$ measurements were performed using a Finnigan MAT CHN-IRMS Finnigan DeltaPlus XP (precision of 0.2‰ and 0.3‰ respectively). Both

instruments are located at the Serveis Cientifico-Tècnics (SCT) of the Universitat de Barcelona (UB).

To investigate the mineralogy and size of the mineral grains present in the levels with higher inorganic content (Margalef et al., 2013), three representative samples were selected; a level rich in Ca and Fe (4.8 m depth), and two silty levels with high values of Ti and Fe (8.3 and 10.55 m depth). These samples were dried and mineral grains were density separated in purified water. The grains were carefully attached to stubs using a conductive bioadhesive tape. A morphological description using a FEI ESEM-EDS in the *low vacuum mode* (around 0.5 torr) and *high vacuum mode* ($< 10^{-4}$ torr) was made on the selected samples in the SCT-UB. Stubs were carbon-coated before being observed in *high vacuum mode*. Secondary and backscattered electron images and Energy-dispersive X-ray spectroscopy (EDS) were used systematically to characterize the mineral grains.

All geochemical sample preparation for Inductively Coupled Plasma-Atomic Emission Spectrometry (ICP-AES) was performed under clean laboratory conditions using acid cleaned labware. Each 250 mg of sample was digested using a mixture of HNO_3/HBF_4 as described by Krachler et al. (2002). The microwave program included a 40 minute several-stage ramp to 200°C where samples were held for 20 minutes. The remaining solution was then transferred to Savillex vessels and evaporated on a hotplate at 50°C. Thereafter H_2O_2 was added and allowed to react for half a day. Samples were then sonicated and evaporated at 50°C. This was followed by a 2 day closed vessel digestion at 90°C with HNO_3. After sonication and evaporation at 50°C an additional cycle of H_2O_2 was made. Samples were once again evaporated and then taken up in 1% HNO_3 for analysis. The samples were analyzed for elemental concentrations using a Varian Vista AX ICP-AES at the Department of Geological Sciences, Stockholm

University, Sweden.

A suite of twenty elements were acquired including Al, Ba, Ca, Cd, Cr, Cu, K, Fe, Li, Mg, Mn, Na, Sc, Sr, Ti, Th, V, Y, Zn and Zr. To date, there is no certified reference material for peat that offers a wide range of elemental data. There is however a peat reference material NIMT/UOE/FM/001 that was tested and analyzed by Yafa et al. (2004). The analytical performance was thus assessed using this material as well as NIST SRM-2711a Montana Soil and NIST SRM-2586 Trace Elements in Soil. Five procedural replicates were made of each reference material. For NIMT/UOE/FM/001, our peat reference material, most elemental recoveries were high, ranging from 99% to 119%. Cadmium however had even higher recoveries (128%) while low recoveries were recorded for Ti (63%). For the other two reference materials, both soils, recoveries were much lower. For NIST SRM-2586 recoveries range from 70-91% for Al, Ba, Ca, Mg, Sc, Sr and Y and 53-66% for Cd, C, Fe, Mn, V and Zn. Again Ti had exceptionally low recoveries (44%) while Th had concentrations double the recommended values. For NIST SRM 2711a recoveries ranged between 64-84% with the exception of Ti (42%) and Th again had concentrations double the recommended values. Replicates of the reference materials were generally within 20% or better of each other. Procedural blanks for were below 3% of the average sample concentrations for the majority of the elements. Slightly higher blanks were found for Al and Mn (<5%), Ba and Cr (<12%) and Zr (<32%).

While the original intention was to make a total digestion of the peat samples, the reference materials suggest that this may not be the case. Although the recoveries for the peat reference material are high, the recoveries for the reference soils are much lower. Nonetheless, in a paleoenvironmental context the relative changes of the elements can still reveal past changes. For this reason all elements, even those with lower (Ti, for

example) or higher recoveries (Th, for example) or potentially high blanks (Zr, for example) were included in our interpretation. Some elements were removed from the dataset because of low concentrations in the peat samples (Li and K), contamination during sampling (Zn) or because the concentrations were close to the analytical detection limits (Na). In the case of Th and Zr particularly, both elements present high communalities in the PCA, suggesting that their signals are not just analytical noise, and their behavior has a coherent paleoenvironmental significance.

Rock and soil analyses

Determination of the elemental composition of rocks and surface soil samples from Rano Aroi and Rano Raraku craters and other parts of the island was performed on 16 samples. All soil samples (5 samples, see supporting information) were obtained from the surroundings of Rano Raraku crater, while rock samples (11 samples, see supporting information) were collected around the Rano Aroi, Rano Raraku craters and other parts of the island. All samples were ground in a ring mill and dried at 60°C for 24 h. Each 0.1 g of sample was then digested using a mixture of 2.5 ml HNO_3+ 5 ml HF + 2.5 ml $HClO_4$ in Teflon tubes at 135°C for 12 h. Finally, 1 ml of HNO_3 and 5 ml of purified water were added to dilute the sample for analysis. The analyses were carried out with a high-resolution ICP-MS (HR-ICP-MS), Element XR Thermo Scientific located at the LabGEOTOP service of the Institute of Earth Sciences Jaume Almera-CSIC (Barcelona). Twenty-three elements were measured. Results are provided in the supporting information (Table 1).

3.2 Pollen analysis

A subset of 25 samples (3-4 g of wet peat) equally distributed along the record were extracted from Rano Aroi peat record and processed for pollen analysis using standard laboratory procedures by Rull et al. (2010b), which include sieving, digestions with

KOH, HCl and HF, and acetolysis. As an exotic marker, one spore tablet of *Lycopodium* (Batch. No. 177745, Lund University, Sweden) per gram was added to each sample before processing. The slides were mounted in silicone oil (not permanents) to be counted under optical microscope using x40 and x60 objectives mounted on a ZEISS® microscope with x10 ocular (ZEISS® Axioplan, ZEISS® Axiostar plus, ZEISS® Axio Scope A1and ZEISS® Axio Lab. A1).

Pollen counting was carried out until at least a total of 200 pollen grains, excluding spores and aquatic and semi-aquatic plants except for samples with very low pollen concentration. Fern spores are presented as a sum of all spore types. The pollen results are presented in percentages excluding spores and aquatic plants. Spores and aquatic plants are represented as a percentage respect the pollen sum. The pollen zonation was performed using psimpoll 4.26 (Bennett, 2002) by optimal splitting (Bennett, 1996). The counting of pollen grains and spores was carried out by comparisons with reference books and atlases for pollen as Hesse et al. (2009); Heusser (1971); Hoeve and Hendriskse 1998; Tryon and Lugardon (1991); Reille (1992); and the online pollen and spore atlas APSA (2007).

Many questions about former flora ecology and distribution of Easter Island remain unsolved, despite that several works have tried to reconstruct vegetation changes from pollen analyses on lake sediments (Azizi and Flenley, 2008; Butler et al., 2004; Dumont et al., 1998; Cañellas-Boltà et al., 2013; Flenley and King, 1984; Flenley et al., 1991; Gossen, 2007) or from macrofossil remains on lacustrine records or archeological sites (Cañellas-Boltà et al., 2012; Dumont et al., 1998; Mann et al., 2008; Orliac and Orliac, 1998; Orliac, 2000; Peteet et al., 2003). As an important number of flora species are now extinct from the island and the native Easter Island flora has been intensely perturbed (Dubois et al., 2013; Rull et al., 2010a), it is not possible to reconstruct

paleoenvironments from pollen analyses using local modern analogues. For this reason, a comparison with other islands (Juan Fernández, Hawaii, Rapa Iti) is useful in order to reconstruct vegetation changes observed in the pollen analysis (see section 4.4 for more information).

3.3 Age-depth model

An age model was built from 19 radiocarbon AMS dates measured from pollen concentrates in the Poznan Radiocarbon Laboratory (Poland) (see Margalef et al., 2013 for full details). Pollen enrichment process followed a classical treatment (Faegri & Iversen, 1989; Moore et al., 1991) modified by Rull et al. (2010b). The AMS ages were calibrated using CALIB 6.02 software, and the INTCAL 98 curve (Reimer et al., 2004) and CalPal (Danzeglocke, 2008) for samples older than 20,000 radiocarbon yr BP. The age model was built by simple linear interpolation between the radiocarbon dates as described in Margalef et al. (2013).

3.4 Statistical analysis

Principal component analysis (PCA) was applied in order to reduce the large ICP-AES dataset to a smaller number of variables. These principal components (PC) could then be interpreted in terms of geochemical and environmental processes. SPSS version 22 statistical software was used to perform the PCA including varimax rotation over the previously logged (ln) and standardized ICP-AES dataset (Al, Ba, Ca, Cd, Cr, Cu, Fe, Mg, Mn, Sc, Sr, Ti, V, Y and Zr).

Correlation coefficients between stable isotopes, organic matter elemental composition and principal components scores were then calculated. To complement the integrative study of all proxies, multiple regression models (stepwise regression mode) using the scores of the extracted principal components (PCR analysis) were obtained for TC, TN, TS, $\delta^{13}C$, $\delta^{15}N$, $\delta^{34}S$ using SPSS version 22 software.

4. RESULTS

4.1 Peat facies and age model

The Rano Aroi core (ARO 06 01) is made up of radicel peat as defined by Succow and Joosten, (2001), consisting of fine roots (diameter < 1mm) with <10% comprising larger remains, from Cyperaceae, Poaceae and Polygonaceae (Margalef et al., 2013). Based on plant type and remain size, geochemistry and degree of peat decomposition, 4 peat facies have been defined (Margalef et al. 2013). **Facies A** (reddish peat) consists of coarse plant remains, with very high C/N (43-111) ratios and $\delta^{13}C$ values between -21‰ and -26‰. **Facies B** (granulated muddy peat) is a light brown peat with low mineral content, made up of coarse to mid-sized organic fragments, mostly roots and rootlets. This facies is characterized by high C/N (41-85) ratios and $\delta^{13}C$ values ranging from -14‰ to -26‰. **Facies C** (organic mud) is found as centimeter thick layers interbedding Facies B. These layers have high mineral contents, high TN (1.08-1.76%) and relatively light $\delta^{13}C$ values (-14‰ to -22‰). **Facies D** consists of dark and fine-grained peat and is highly decomposed (pictures of the described facies can be found in Margalef et al., 2013).

The age model revealed large changes in peat accumulation rates and the occurrence of a long hiatus in the sequence (see supporting information, Table 2). (1) The bottommost part of the sequence (8.75 m -13.9 m) was accumulated prior to 55 kyr BP and, in consequence, it is beyond the limits of radiocarbon dating. Because the accumulation rate between 55 and circa 40 cal kyr BP (3.7–8.72 m) is almost constant and the peat facies are the same until the base of the sequence, we make the initial assumption that accumulation rates were also relatively constant for the bottommost part of the sequence. Consequently, this part of the sequence has been dated by extrapolation using the accumulation rate of the upper section (3.7–8.72 m) of the core

sequence (see Margalef et al., 2013 for further details). (2) A sharp unconformity occurs at 4.25 m (39 cal kyr BP), where highly oxidized peat (Facies D) is overlaid by much less decomposed peat (Facies A). Dating results, the peat facies D and the biogeochemistry data suggest that during a certain period of time after 39 kyr cal BP the wetland underwent a long-term drought (with likely associated peat decomposition and loss) resulting in a subaerial exposure (Margalef et al., 2013). (3) Above the clear unconformity, our age model shows extraordinary low peat accumulation rates, and 16,000 years are represented by 104 cm (between 3.27 m and 4.31 m, see table 2 from supporting information).

4.2 Geochemistry on peat cores

4.2.1 Organic geochemistry

Total C concentrations are highly variable but without any specific trend, ranging from 40% to 70% (Fig. 2). $\delta^{13}C$ shows constant values around -14 ‰ between 14 m and 9 m shifting gradually to values around -26‰ from 9 m to 6 m, and staying around these more negative values for the uppermost five meters of the sequence. In addition to the long-term trend, the $\delta^{13}C$ curve also shows high-frequency changes (dips) and significantly lower values for Facies C between 11 m and 6 m (Fig 2 and 6; Margalef et al., 2013). Total N contents range between +0.5% and +1.75%. C/N ratios are between 33 and 111. $\delta^{15}N$ values oscillate between -2.03 and +8.87‰. Peat sections with the heaviest isotopic composition, above +8‰, are found at 12.4 m and 10.7 m depth and above 6 ‰ at 3.40 m depth (Fig. 2).

Total S values are low (less than 1%) and show a decreasing trend from the bottom of the core to 6 m depth, followed by a slight increase from this depth to the top of the core. On the other hand, the $\delta^{34}S$ record can be divided into two main sections: below 8 m the average value is +18.04 ± 0.88 ‰ and above this depth it is +19.33 ± 1.60‰. The

shift between the two sections occurs at 7.7-7.2 m. (Fig. 2).

4.2.1 Mineral grain found on peat cores geochemistry

Most of the mineral grains observed under electronic microscope showed evidence of transport or advanced weathering. At 8.3 m and 10.55 m depth small grains (30-500 μm) were rutile, ilmenite and quartz, while the bigger grains (≥500 μm) were composed of inosilicates (pyroxenes), plagioclases and quartz. The sample from 4.8 m depth showed smaller grains (10-20 μm) composed of iron, magnesium and aluminum oxides, quartz and organic compounds bound to Ca, Br and Mg. Some of these organic compounds were large up to 200 μm.

4.3 Rock and soil analyses

The elemental composition of selected rock and soil samples from the Rano Aroi watershed and other areas of the island was analyzed to investigate the origin of the inorganic fraction arriving to the mire. The ICP-MS analyses show that basalt, hawaiite and tholeiite rocks are especially rich in Fe_2O_3 (16-22%) and TiO (2.5-4.4%) (see supporting information Table 1) as documented by previous petrographic studies (Baker et al., 1974). The other major components are found in the following concentrations: Al_2O_3: 16-22%, MnO: 0.3-0.5 % and CaO: 3.3-9%. Minor and trace elements showed the following ranges: Sc: 24-39 μg g^{-1}, V: 170-500 μg g^{-1}, Co: 40-163 μg g^{-1}, Cr: 1-60 μg g^{-1}, Ni: 2.2-29.5 μg g^{-1}, Cu: 16-112 μg g^{-1}, Zn: 110-185 μg g^{-1}, Sr: 76-280 μg g^{-1}, Y: 40-85 μg g^{-1}, Zr: 276-497 μg g^{-1}, Ba: 107-202 μg g^{-1}, Th: 2.4-5.2 μg g^{-1} (Table 1 of supporting information). The rock samples around Rano Aroi are particularly enriched in Ti, Al, Sc, V, Cr, Ni, Cu and depleted in Y, Zr, and Ba, when compared to samples from other areas of the island. On the other hand, the Easter Island andosols sampled for this study were especially enriched in Al, Cr, Y, Zr and depleted in Mg, Ca, Sc, V, Co, Ni, Cu, Zn, and Sr compared to rock samples.

4.4 Peat ICP-AES data and PCA

A PCA was performed using the suite of selected elements from the bulk peat analysis. Three components explaining 85% of the matrix variance were identified. The absolute concentration variations for elements representative of these PCs are shown in Fig. 2. The results of the PCA are presented in terms of the factor loading of each element in the extracted PCs by showing the fractionation of the communalities (i.e., the proportion of the variation of each variable explained by each PC) (Fig. 3) and by the depth records of the PCs factor scores (Fig. 4). The first component (PC1, 40.8% of the variance) is tied mainly to V, Al, Sc, Cr, Cd and Y (with positive loadings between 0.71 and 0.93, Al shown in Fig. 2) and to a lesser extent to Ti, Zr, Cu and Mn (Ti and Zr shown in Fig. 2, communalities shown in Fig. 3). The second component (PC2, 23.1% of the variance) is characterized by large positive loadings (between 0.69 and 0.93) of Th, Fe, Mn and Ba (Fe shown in Fig. 2) with significant contributions from Ti, Zr and Sr (Ti and Zr shown in Fig. 2, communalities shown in Fig. 3). And the third component (PC3, 21.3% of the variance) is characterized by large positive loadings (between 0.87 and 0.94) of Mg, Ca and Sr and moderate ones of Cu and Ba (Ca shown in Fig. 2, communalities shown in Fig. 3).

PC1 shows high scores in the older section of the peat record (>55.5 kyr BP; 9 m). A clear shift from higher to lower values is observed between 55.5 and 41.5 cal kyr BP (9-5.16 m), followed by a rapid increase until 31cal kyr BP (3.76 m) and stabilization thereafter (Fig. 4). PC2 variability shows a peaky pattern. From the bottom of the core to 6.1 m PC2 scores present peaks at 10.6 m, 10.01 m, 8.7 m and 7.73 m. From 6.1 m to 4.8 m values become high and quite stable, then start to decline gradually until 2.96 m (Fig. 4). Two prominent peaks occur in this last interval (4.8-2.96 m): at 4.05 m and at 3.45 m, the latter being the maximum of the entire record. At the upper

part of the sequence, from 2.96 m to 2.40 m PC2 shows a progressive increase. The PC3 scores do not show a clear trend at the bottom of the sequence. From 10.49 m to 8.15 m there is a clear declining trend, and a marked see-saw pattern until 5.79 m. Scores rapidly increase from 5.79 m to 5.41 m, defining a broad peak up to 4.25 m. From 4.25 m to 3.16 m PC3 scores decline irregularly, but a clear peak stands out in this interval at 3.86 m. The uppermost part of the sequence presents an increasing trend, (Fig. 4).

4.5 Pollen record

In this work, only the most abundant taxa: Poaceae, *Arecaceae* , Asteraceae, *Coprosma* and Cyperaceae pollen types together with fern spores sum have been used. The following taxons are included as "others": Triumfetta, Acalypha, Trema (Ulmaceae), Pinus, Macaranga, Sapinus, Plantago plus indeterminate and unknown pollen types.

Asteraceae (arbustive types) are present in Hawaii, Rapa and Juan Fernandez Island although nowadays these are not found on Easter Island, (Brown, 1935; Flenley et al., 1991, Zizka, 1991). In Hawaii these small trees form scarce-forested landscapes in between true forest and bare lava flows (Flenley, 1991). Native and endemic Poaceae are mainly present in meadows and open landscapes. Some biogeographical and ecological constraints of the known species are given in Table 3 of the supporting Information. Based on the endocarp of fossil seeds, an endemic species of Arecaceae tree has been proposed: *Paschalococos disperta* (Dransfield et al., 1984). This endemic species is extremely similar to *Jubaea chilensis* (Dransfield et al., 1984, Flenley et al., 1991*)* and is presented as an emblematic case of extinction. *Coprosma* is a genus of flowering plants (small trees) present on many Pacific sites (New Zealand, Hawaii, Borneo, Rapa, Juan Fernández). It is nowadays completely extinct from Easter Island but found in ancient lake and peat sediments (Flenley, 1991; Horrocks et al., 2013).

Cyperaceae is another abundant pollen type predominantly representing taxa found in moist and waterlogged parts of grassland meadows or peatlands (supporting information, Table 3). Finally, fern spores also constitute an important part of Rano Aroi pollen record, in contrast to the low dominance of fern spores observed in Rano Raraku lake sediment cores (Cañellas-Boltà et al., 2013; Flenley et al., 1991).

Two significant zones were obtained (Fig.5) over the complete pollen dataset:

Zone I (13.9-7.48 m depth, 71-48.3 kyr BP) is characterized by the dominance of Poaceae (70-90%) with an important contribution of *Arecaceae*, *Coprosma* pollen and fern spores.

Zone II (7.48-2.35 m depth, 48.3-8.5 kyr BP) is defined by an increase of Asteraceae at the expense of Poaceae and Arecaceae pollen. The appearance of a higher amount of Cyperaceae, probably from the mire itself, is remarkable. The elevated number of fern spores indicates that these might have been growing in the vicinity of the mire. Cyperaceae as other aquatic and semiaquatic plants can be useful to determine local conditions because they grow specifically in moist and flooded areas. Because of the strong local signal they are not included in the sum to perform percentages.

This Zone has been divided in three subzones in the following manner:

-Zone IIa (7.48-5.8 m depth, 48.3-43 kyr BP): this subzone is characterized by very high percentages of Asteraceae pollen (up to 70.5% at 6.15 m depth) while Poaceae pollen percentage remains lower than in Zone I. Fern spores start to be more abundant, together with Cyperaceae that depict increasing percentages from bottom to top of the zone.

-Zone IIb: (5.8-3.4 m depth, 43-20.6 kyr BP). The subzone consists of a pollen assemblage with a lower percentage of Asteraceae and a higher contribution of Arecaceae , Cyperaceae and fern spores. This subzone also contains a hiatus at 4.25 m

(see section 4.1).

- Zone IIc (3.4-2.35 m depth, 20.6-8.5 kyr BP) is characterized by a considerable reduction in Asteraceae and the dominance of Cyperaceae and ferns.

4.6 Correlation between inorganic and organic peat chemistry

In the PCA described above we did not include the variables that characterize the chemical nature of the organic matter, because our main objective was to determine the chemical nature of the minerogenic fraction in the peat. The next step is to correlate the first three PC with the chemical composition of the peat organic matter (TC, TN, TS, and the isotopic composition) to look for covariance and to investigate the underlying processes controlling the changes in peat inorganic and organic matter, and how external and internal (i.e. postdepositional) processes have affected both the inorganic and the organic chemistry. The largest correlation values (Table 1) were found between PC1 scores and TN, C/N ratios, $\delta^{15}N$, $\delta^{13}C$ (r are 0.66, -0.62, 0.65 and 0.59 respectively). Lower, but significant correlations ($p<0.01$) were found between PC1 and TS ($r = -0.45$), PC2 and $\delta^{13}C$ ($r = -0.31$), and PC3 and TC, C/N ratios and TS (r are 0.30, 0.32 and 0.35 respectively, Table 1).

This relatively weak correlation structure may indicate that peat organic chemistry was mainly controlled by factors other than those governing the observed changes in the inorganic chemistry. But it may also reflect that there was no single dominant control and that all or a combination of factors is responsible for peat geochemistry. To check the latter possibility we performed a multiple regression analysis using as input variables the three extracted principal components. Such a multiple regression models is called principal components regression, PCR (see for example Desta Fekedulegn et al., 2002). The results of the PCR models can be found in Table 2. As expected, the models show larger correlation coefficients. Nevertheless, TC and $\delta^{34}S$ show a low ($R = 0.35$

476 and R = 0.49, respectively) and TS only a moderate correlation (R = 0.66) with the
477 principal components, which may be taken as evidence that C and S cycling in Rano
478 Aroi was not only coupled to the main processes responsible for the changes in the
479 inorganic chemistry. On the contrary, TN, C/N ratios, $\delta^{13}C$, and $\delta^{15}N$ show significantly
480 larger correlation coefficients (R = 0.72-0.75). For these variables PC1 has the highest
481 regression coefficients (positive for TN, $\delta^{13}C$, and $\delta^{15}N$, and negative for the C/N ratio;
482 Table 2) and is thus the most influential. A visual representation of the adjustment of the
483 predictive models to the original data can be found in the Figure 1 of the supporting
484 information. For TN and C/N ratios the similarity of the records of observed and
485 expected values are quite remarkable, while for $\delta^{13}C$ and $\delta^{15}N$ the model basically
486 accounts for the long-term changes but not for the short term events. For TS the fitting
487 between real and expected values is pretty good except for the section comprised
488 between 6.34 and 5.54.

489 **5. DISCUSSION**

490 **5.1 Factors controlling peat elemental composition**

491 The PCA performed on the Rano Aroi inorganic elemental dataset identified three
492 main components that enable an identification of specific variables for each component
493 (i.e., chemical elements in this case) whose behavior is similar and, thereby, likely
494 controlled by the same process (Reimann et al., 2008).

495 *5.1.1. Long-term mineral fluxes of very fine particles*

496 PC1 is characterized by large positive loadings (>0.7) of typically lithogenic
497 elements (V, Al, Sc, Y, Ti, Zr*)* and some metals (Cr, Cd, Cu). These elements are
498 associated with very fine particulate material and this component can confidently be
499 related to the deposition of soil dust transported by wind together with contributions
500 from hydric erosion. Given the isolation of Easter Island, this signal would be mainly

501 dominated by fluxes from the volcanic rocks and soils of the island itself. Elements on
502 this first component (like Al, Ti, Zr, Cr, Cu and other metals) are enriched in volcanic
503 soils with increasing degree of pedogenesis (Martínez Cortizas et al., 2007a). Almost
504 the same association of chemical elements (V, Al, Ti, Sc, Cu) was found by Muller et al.
505 (2008) in the study of the composition of the Lynch's Crater, a mire in NE Australia
506 with remarkable similarities with Rano Aroi (both mires are minerotrophic and formed
507 within a volcanic crater). The weathering of volcanic materials leads to the distribution of
508 this association of elements in (1) secondary minerals or organo-metallic compounds,
509 which are poorly crystalline or in (2) primary minerals, which are very resistant to
510 weathering. Most of these mineral phases are characterized by very fine (probably ≤ 50
511 μm) particles, which are easily mobilized by eolian or hydric erosion. This is consistent
512 with what is found after SEM observations on the Rano Aroi record because particle
513 size (except for Facies C) was dominated by fine silt and clay fractions (<30 μm).
514 Therefore, PC1 would track the long-term *background* fluxes of inorganic particulate
515 material coupled to soil pedogenesis and erosion (and factors affecting both). Fine
516 airborne dust particles are enriched in many elements compared to coarser ones
517 (Schuetz, 1989), and these chemical processes lead to potential physical and chemical
518 fractionation during dust transport, which seems to be more intense at short distances
519 from the source area and attenuates during long-range transport, as the grain size of the
520 dust decreases and homogenizes. The elemental composition reflected by PC1 is
521 consistent with these chemical enrichment processes associated to dust input variability.
522 *5.1.2 Strong runoff events and coarser detrital input*
523 The second component, PC2, is characterized by large positive loadings of Fe, Mn
524 and Ba and moderate positive loadings of Ti and Zr. These elements are associated to
525 coarser particles entering the mire. Non-systematic Scanning Electron Microscopy

526 (SEM) observations of the peat layers corresponding to high PC2 scores showed an
527 abundance of sand (50-600 μm) and coarse silt (20-50 μm) particles.

528 Iron and Mn are elements which can show a strong redox behavior, tending to be
529 depleted under anoxic conditions due to the mobility of their reduced forms and
530 accumulated under oxidizing conditions in peatlands (Chesworth et al., 2006;
531 Steinmann and Shotyk, 1997). Furthermore, PC2 variability (and the elemental profiles,
532 Figure 2) does not show a long-term trend as documented for redox sensitive elements
533 (i.e. Fe or Mn) in the Lynch's Crater record (Muller et al., 2008). However, the Rano
534 Aroi record has rather a peaky pattern resembling an "event signal". Despite its
535 potential mobility, Fe has been found to be immobile in certain peatlands (Muller et al.,
536 2008; Weiss et al., 2002) and previously formed Fe oxides/hydroxides were found to be
537 stable in lake sediments even under anoxic conditions (Gälman et al., 2009).
538 Additionally, in most soils developed on volcanic rocks such as those in the Rano Aroi
539 catchment, Fe is largely hosted by primary minerals and the Fe that is released during
540 weathering accumulates as non-crystalline or poor crystalline Fe forms (i.e. ferrihydrite,
541 Fe-organic matter associations) and secondary Fe phases (oxides and hydroxides)
542 (García-Rodeja et al., 2007). Barium, Ti, Th and Zr have only one oxidation state and
543 are not sensitive to redox changes, and major hosting minerals of Ba (barite, witherite),
544 Ti (ilmenite, rutile) and Zr (zircon, baddeyelite) are highly resistant to weathering. Thus,
545 in Rano Aroi PC2 is not likely to reflect diagenetic changes associated to changes in
546 redox conditions. Instead, while PC1 reflects the long-term particulate terrigenous input
547 into Rano Aroi, PC2 most likely represents strong, highly erosive runoff events capable
548 of transporting solid particles by suspension or eventually traction to the center of the
549 mire. Peaks in PC2 scores coincide with the presence of Facies C, organic mud, which
550 has been interpreted as being representative of wet events and higher water table levels

551 in the mire (Margalef et al., 2013).

552 *5.1.3 Post-depositional enrichments*

553 PC3 is characterized by large positive loadings of Ca, Sr, and Mg. These elements
554 are transported to the mire included in very fine soil particles (as primary minerals such
555 as plagioclase), but because they are also highly mobile as ions, they are transported to
556 the mire as dissolved species, too. Due to their chemical mobility, groundwater can also
557 greatly contribute to their distribution, sometimes by diffusion from the underlying
558 sediments as a result of the chemical dissolution of Ca-bearing minerals (Shotyk et al.,
559 2002). And, as essential nutrients, they are also subjected to intense biocycling.

560 The most prominent feature of the PC3 record is the maximum values (Fig. 4, Fig. 6,
561 Fig. 7) attained between ca. 42-39 kyr BP (4.25 m and 5.41 m depth) coinciding with
562 facies D (highly decomposed peat, Margalef et al., 2013). Age model, geochemistry and
563 the sharp discontinuity described at the uppermost limit of facies D suggest that there
564 was a loss (i.e. erosion) of previously accumulated peat layers. This would also mean
565 that the geochemical features exhibited below this sedimentary hiatus (between 5.41 m
566 and 4.25 m depth) were acquired thousand years later than accumulation, as diagenetic
567 changes caused by peat aereal exposure. Given this circumstance the most likely
568 explanation for enrichment on facies D was an intensive use of these elements as
569 bio nutrients by the plant community because a more intensive input of Ca, Mg and Sr
570 as a solute form would require a wetter climate. The lowering of the mire water table,
571 due to drought phases, is known to accelerate peat decomposition (Ise et al., 2008) and
572 produce an enrichment of certain elements in the peat (Biester et al., 2012; Martínez
573 Cortizas et al., 2007b). The increase of Ca –among other elements- at surface levels
574 when peat growth stagnates has been explained by Damman et al. (1992) as an effect of
575 the detritus cycle. At Lynch's Crater, Ca, Sr and Mg were also enriched in the more

576 decomposed peats (Muller et al. 2008). Another example of similar chemical
577 enrichments comes from a Canadian mire composed of a 153-cm-thick layer of
578 ombrotrophic, moderately decomposed peat overlying highly humified, minerotrophic
579 peat: Ca was enriched 10 fold; Mg 2-3 fold; Fe (3 fold) in the highly decomposed peat
580 (Zoltai and Johnson, 1985). In Rano Aroi the maximum concentrations for Ca, Mg and
581 Sr in the c. 42-31 kyr BP (6-4 m depth) peat are around 5 fold, 3 fold and 2.5 fold higher
582 than average concentrations in the peat deposited ca. 55-42 kyr BP (8-6 m).

583 ***5.2 Linking the organic and inorganic peat chemistry***

584 *5.2.1 PC1 and organic chemistry*

585 The long-term variability of PC1 is similar to the long-term evolution of the $\delta^{13}C$
586 record from 55.5 to 43.9 kyr BP (9-6 m, Fig. 6) where both curves have a declining
587 trend. The $\delta^{13}C$ trend shows a shift from values typical of C_4 plant types to lighter ones
588 (characteristic of C_3 type) and suggests a change in the peat forming plant community
589 (Margalef et al., 2013). This synchronicity between $\delta^{13}C$ and PC1 reveals an intimate
590 relation between soil evolution and vegetation cover (see section 5.3).

591 The TN content decreases in the upper part of the sequence (Fig. 6) suggesting a link
592 with soil evolution (PC1) and vegetation cover ($\delta^{13}C$). $\delta^{15}N$ (Fig. 2) can provide
593 information on organic matter origin, nitrogen fixation ($\delta^{15}N$= 0 to +3 ‰) or plant
594 productivity, but also syndepositional processes such as denitrification ($\delta^{15}N \geq +8$ ‰)
595 (Handley et al., 1999; Meyers and Ishiwatari, 1993; Talbot and Johannessen, 1992). At
596 Rano Aroi the average $\delta^{15}N$ is around +2.7 ‰, which is an isotopic signature typical of
597 nitrogen fixation. The general $\delta^{15}N$ trend correlates directly with PC1 variation, as
598 denoted by the high PCR regression coefficient (R= 0.56). Two hypotheses can be
599 proposed to explain this relationship: (1) larger inputs of fine or very fine mineral
600 particles to the mire may have triggered conditions of enhanced productivity and

consequently, higher $\delta^{15}N$ values; or (2) the vegetation change can entail a differential fractionation of the peat forming plant remains (Talbot, 2001). However, two prominent peaks of $\delta^{15}N$ at 66.8 kyr BP and 62.4 kyr BP (12.36 m and 11.07 m, Fig. 1 from supporting information) are not accounted for by the PCR model and thus, they are apparently not related to the influx of mineral matter or long term shifts (supporting information, Fig. 1). These very high $\delta^{15}N$ values ($\delta^{15}N \geq 7$ ‰) may have been reached by the preferential loss of light nitrogen through denitrification or ammonization (Talbot et al., 2001) indicating anoxic phases. Therefore, our results suggest that different processes could change the isotopic signature over different time scales: long-term variability related to a shift in the vegetation and short-term variability related to small-scale events such as a change in the potential redox.

Total S (decreasing) and $\delta^{34}S_{CDT}$ (increasing) trends from 55.5 to 43.9 kyr BP (9-6 m) also show a differential S assimilation and fractionation through time (Fig. 2). The changes in S cycling, especially $\delta^{34}S_{CDT}$, seem partially related to PC1 and the shift in $\delta^{13}C$ (Table 1). Sulfur is incorporated by plants and bacteria, especially in the form of organosulfur compounds, which seem to be the dominant S fraction in peat (Novák et al., 1994 and 1999; Wieder and Lang, 1988). The chemical composition of the Rano Aroi basin lithology indicates that inorganic S-content is low or negligible and this is not considered a source of S to the mire (Baker et al., 1974, Margalef et al., 2013). Because no volcanic eruption has been recorded nor have ash layers have been described in Rano Aroi and Rano Raraku in late Quaternary sediments (Flenley 1991, Sáez et al. 2009) the most likely dominant S source is marine sulphate. Variations in TS and $\delta^{34}S_{CDT}$ can be therefore explained as changes in the loss after early diagenesis (bacterial sulphate reduction and fixation) that discriminates against the heavier isotope ^{34}S (see supporting information for additional information about sulphur interpretation).

626 *5.2.2 PC2 and organic chemistry*

627 PCR analyses show that organic matter composition does not significantly
628 correlate with PC2; however, several cause-effect relationships can be drawn from
629 the stable isotope, TC, and TN records. $\delta^{13}C$ second order changes (i.e. peaks) show
630 lower values coinciding with Facies C and PC2 peaks from the bottommost part of
631 the record until 6 m depth (Fig. 6). This relationship between organic matter and
632 Facies C can be explained by differential fractionation due to moisture changes or a
633 higher proportion of C_3 plants during wet events (Margalef et al., 2013). Abrupt
634 increases of TN also match PC2 peaks (Fig. 6). High TN values together with low
635 C/N ratios can be attributed to a higher contribution of lacustrine algal material
636 (low C/N), in contrast to high C/N values that indicate higher proportions of
637 terrestrial or aquatic plants (*versus* algae) organic matter (Meyers, 1994).

638 *5.2.3 PC3 and organic chemistry*

639 The organic chemistry does not correlate with PC3. Nevertheless, the drought event
640 may have partially determined the $\delta^{13}C$ signature like the lighter ratios on the highly
641 decomposed part of the record show. The same can be stated for the C/N ratios that are
642 slightly higher between 5 m and 4.23 m depth (Fig. 2). Total S displays a relative
643 enrichment between 5 m and 4.23 m depth while the underlying level, from 6.5 m to 5.5
644 m depth, becomes depleted in S. This pattern could respond to bioaccumulation through
645 the formation of organic S compounds that are more stable under oxidizing conditions
646 at the expense of the S released from the layers that remained under reducing conditions
647 near the watertable interphase (coherently when $\delta^{34}S_{CDT}$ reaches the maximum values).

648 ***5.3 Rano Aroi environmental reconstruction: climate, basin and peatland***
649 ***interactions***

650 The Rano Aroi dataset and our multi-proxy approach allow us to reconstruct

651 paleoenvironmental changes considering the intimate interplay between climate forcing,
652 basin and catchment evolution (soil and vegetation changes) and peat processes.
653 MIS 4 (73.5-59.4 kyr BP) is a period characterized by low southern Pacific SST
654 temperatures (Kaiser et al., 2005, Pena et al., 2008, Fig. 7H). The Antarctic Circumpolar
655 Current (ACC) was enhanced and the Southern Westerlies moved equatorward resulting
656 in sea ice export away from Antarctica (Kaiser et al., 2005). Sea level was globally low,
657 between 90 and 100 m below the present day (Grant et al., 2012, Fig. 7E), which has
658 been proposed as an important factor for Easter Island's hydrology and groundwater
659 levels as well as that of other small islands (Margalef et al., 2013). A lower sea level
660 would probably also cause lower groundwater levels. This time period sees a complete
661 dominance of C_4 plant types (mostly Poaceae) on the Rano Aroi basin and Terevaka
662 area (Fig. 6) and the presence of Arecaceae and *Coprosma* taxa on the island. Some
663 studies have proposed the development of palm tree forests preferentially in the lower
664 areas of the island (Flenley et al., 1991), although other authors suggest that the
665 palynological results obtained so far are also coherent with a mosaic vegetation pattern
666 with forested areas around permanent mires, lakes and the coastline as gallery forests
667 (Rull et al., 2010a).
668 The prevalence of C_4 plants suggests drier conditions that would lead to a low degree
669 of pedogenesis in the catchment soils; a scenario that is coherent with the low global
670 temperatures (Grant et al., 2012; Kaiser et al, 2005; Fig. 7H and E). Additionally,
671 herbaceous plant dominance may have facilitated higher soil erodibility, either eolian
672 and/or hydrological. The result was a higher dust flux of typical lithogenic elements and
673 metals into the mire, as summarized by PC1.
674 Globally warmer conditions heralded the arrival of MIS 3 (59.4-27.8 kyr BP). SST of
675 mid latitudes of Pacific Ocean increased around 5°C between 62.7 and 61.5 kyr BP

676 (Fig. 7H). This change was coupled to a rapid sea level rise, and between 62.9 and 61.2
677 kyr BP sea level shifted from -96 m a.s.l to -75 m a.s.l (Grant et al., 2012). In the South
678 Pacific, atmospheric patterns underwent important reorganizations. A record from the
679 Cariaco Basin (Peterson et al., 2000, Fig. 7F) indicates that between 61.2 and 59.9 kyr
680 BP the Intertropical Convergence Zone (ITCZ) was situated in a stable southern
681 position leading to very dry conditions in Northern Hemisphere tropics. The southern
682 latitudinal migration of ITCZ therefore leads to the opposite hydrologic trend for the
683 low latitudes in the Southern Hemisphere (Leduc et al., 2009; Wang et al., 2007,). The
684 early MIS3 has been characterized in the Rano Aroi record as a humid period, as
685 expressed by the abrupt events of higher sediment delivery (see section 5.1.2, and Fig. 6
686 and 7). It is significant that the first important wet event on Easter Island, starting in
687 Rano Aroi at 61.6 kyr BP is apparently synchronously with important global changes in
688 (1) sea level rise, (2) the position of the ITCZ and (3) SST.
689 The new warmer and wetter conditions of Early MIS 3 (61.6 to ~40 kyr cal BP) were
690 linked to an intensification of the degree of pedogenesis, which led to a decrease in the
691 flux of lithogenic elements to the mire. In parallel to the decline in PC1 values (Fig.
692 7B), the bulk peat stable isotope data values ($\delta^{13}C$ and $\delta^{15}N$) started a gradual decline at
693 55 cal kyr BP (Fig. 6). The isotopic change indicates a shift in the vegetation
694 community forming the peat, which becomes dominated by C_3 plant types. As stated in
695 previous sections, pollen data suggests that a complete dominance of Poaceae
696 (presumably C_4 species) was replaced by a combination of Asteraceae, *Coprosma*,
697 Poaceae and ferns between 51 and 48 kyr BP (Fig. 5). The vegetation change around the
698 mire and the presence of scarce forest, trees and shrubs may have prevented soil erosion
699 and reduced the fluxes of mineral matter to the mire (PC1). Finally, the expansion of
700 Cyperaceae (presumably C_3 species, such as *Scirpus californicus*) probably constituted

701 an important physical barrier during the C_3 dominance period, slowing the runoff input,
702 except during stronger events (PC2).
703 The late MIS 3 (40-27.8 cal. kyr BP) has been characterized as a drier phase on
704 Easter Island (Margalef et al., 2013). Sea level dropped relatively rapidly between 31.4
705 and 29.4 cal. kyr BP, but a South Pacific thermal response to global cooling was not
706 recorded until the onset of MIS 2 (Kaiser et al., 2005, Fig. 7H). The Cariaco Basin
707 record shows that between 35 and 31 cal. kyr BP, the ITCZ was in a northern position
708 preventing the arrival of strong storms to southern latitudes (Peterson et al., 2000, Fig.
709 7F). Moreover, several records from South America document intense dry between ca.
710 41 and ca. 31 cal. kyr BP (Lamy et al., 1998; Stuut and Lamy, 2004) explained by the
711 southern migration of the Southern Westerlies under the precession forcing (Fig. 7G).
712 The combination of these regional climate patterns likely led to a long dry period in the
713 Central Pacific and on Easter Island. The drought started after 39 cal. kyr BP, the age of
714 the sharp unconformity in the Rano Aroi sequence that separates highly degraded
715 (below) and fresh peat (above). A lowering of the Rano Aroi water table accelerated
716 peat decomposition producing an increase in the elements representative of PC3 (Ca, Sr,
717 and Mg) as a diagenetic imprint (Fig. 7D). The time interval above the discontinuity
718 depicts net accumulation rates of 0.05 mm/y (Fig. 7A) and represents the reactivation of
719 peat formation after a long-term pause (probably including erosion) where old carbon
720 could be incorporated in younger roots and plant remains. Because of this carbon
721 recycling, the chronology right after the reactivation has to be carefully considered and
722 the exact date of the reactivation and the amount of peat eroded cannot be properly
723 determined.
724 Although sea level reached a minimum ca. 23 cal. kyr BP (Grant et al., 2012;
725 Lambeck and Chappell, 2001; Fig. 7E) and could have negatively affected the

groundwater input and the hydrological balance at Rano Aroi, peat formation was active during the LGM. These can be explained by permanent cold conditions preventing strong evaporation (Sáez et al., 2009) and a northernmost position of Southern Westerlies whose influence reached subtropical latitudes during glacial times (Lamy et al., 1998, Fig. 7G).

Rano Aroi peat accumulation reactivated completely by ca. 17.5 kyr BP (the onset of Termination 1). Sea level started a prominent rise and the Intertropical Convergence Zone shifted to its furthermost south position between 21 and 16 kyr BP (Fig. 7F). During MIS 2 (27.8-14.7 cal. kyr BP), PC3 values remained low, showing no evidence of a drought period. Conversely, high PC2 events are found during the late glacial at 20.9-19.5 cal. kyr BP and 16.4 cal. kyr BP, likely representing enhanced precipitation coinciding with HS 2 and 1 (Fig. 7C). Maximum peat accumulation rates (14 cal kyr BP, Fig. 7A) coincide with the highest rates of sea level rise during deglaciation (Dickinson, 2001; Hanebuth et al., 2000; Lambeck and Chappell, 2001). Sea level rise together with warmer SST might have played an important role in the development of enhanced convection storms.

According to several Southern Hemisphere records the Early Holocene was characterized by a warming (Pena et al., 2008) and SST were maximal at approximately 12 cal kyr BP and generally decreased thereafter until modern SST were reached (Kaiser et al., 2005; Kaiser et al., 2008). In ARO 06 01 record, only the early Holocene (11.7-8.5 cal kyr BP) peat remains because the surface levels were rejected to avoid anthropic remobilization. The most important features characterizing this period are high PC2 values around 10.2 cal kyr BP indicating strong runoff events, while PC1 points to catchment soil conditions similar to those recorded ca. 48 kyr cal BP indicating relatively low fluxes of inorganic material under a permanent C_3 plant dominance (as

751 shown by $\delta^{13}C$, Fig. 6 and 7).

752 **6. CONCLUSIONS**

753 The organic matter composition (TC, TN, TS, $\delta^{13}C$, $\delta^{15}N$, $\delta^{34}S$), inorganic
754 geochemistry and pollen data from Rano Aroi mire provide a coherent reconstruction of
755 the paleoenvironmental history of Easter Island.

756 Principal components analysis of peat geochemistry reveals that three main
757 environmental processes have controlled the inorganic elemental composition of the
758 peat accumulated. (1) The first process, depicted by PC1, reflects changes in the basin
759 background erosion and transport of the mineral matter as very fine particles into the
760 mire and it is linked to soil evolution and vegetation shift. In Rano Aroi, $\delta^{13}C$ can be
761 used to infer an important vegetation change from C_4 to C_3 plant dominance that
762 occurred from 55 to 50 kyr BP. The correlation of the $\delta^{13}C$ and PC1 records reveals that
763 vegetation shifts and the evolution of the soils of the mire basin were intimately related
764 to the rate of allochtonous material transported into the peatland. These environmental
765 changes also affected the $\delta^{15}N$ signal that integrates variability in mire productivity and
766 redox conditions. $\delta^{34}S$ signatures indicate that the S source is primarily marine. The $\delta^{34}S$
767 ratio and TS concentration suggest that S may have been differentially mobilized
768 depending on vegetation assemblages by sulphate reduction bacteria. (2) The second
769 process is the occurrence of high precipitation events (identified by the PC2 signal)
770 related to strong runoff and delivery of large amounts of terrigenous particles coarser
771 than those mobilized by PC1 process. These events occurred at approximately 60 kyr
772 BP, 52 kyr cal BP and 42 kyr cal BP. (3) Finally, the third process, illustrated by PC3,
773 mainly reflects peat oxidation caused by a long-term drought after ca. 39 kyr cal BP.

774 The environmental evolution of Rano Aroi mire, largely driven by hydrological
775 changes, is coherent with the regional climatic variability described for the last 70 kyr

776 BP. During MIS 4 the Rano Aroi basin was occupied by open grasslands and C_4
777 Poaceae dominated the mire owing to the generally cold and relatively dry climate
778 conditions. MIS 3 was marked by the onset of wet events, which occurred at ca. 60 kyr
779 BP, 52 kyr cal BP and 42 kyr cal BP.
780 During the first half of MIS 3 and probably driven by the wetter and warmer
781 conditions, Asteraceae and other small trees became gradually more abundant, forming
782 scantily wooded areas around Terevaka, while C_3 peat forming plants colonized the Aroi
783 mire. In contrast, the second half of MIS 3 was drier. A long-term drought led to a water
784 table drop and enhanced peat mineralization at some time between the 39 and 31 kyr cal
785 BP. During the MIS 2 and LGM the water table recovered and peat accumulation
786 resumed under C_3 plant dominance.
787

AKNOWLEDGEMENTS

This research was funded by the Spanish Ministry of Science and Education through the projects LAVOLTER (CGL2004-00683/BTE), GEOBILA (CGL2007-60932/BTE) and CONSOLIDER GRACCIE (CSD2007-00067) and an undergraduate grant JAE (BOE 04/03/2008) to Olga Margalef. We would like to thank CONAF (Chile) and the Riroroko family for the facilities provided on Easter Island.

795 References

796 APSA Members* (2007) The Australasian Pollen and Spore Atlas V1.0. Australian
797 National University, Canberra. http://apsa.anu.edu.au/

798

799 Aucour, A. M., Bonnefille, R., Hillaire-Marcel, C., 1999. Sources and accumulation
800 rates of organic carbon in an equatorial peat bog (Burundi, East Africa) during the
801 Holocene: carbon isotope constraints. Palaeogeography, Palaeoclimatology,
802 Palaeoecology 150, 179–189.

803

804 Azizi, G., Flenley, J.R. 2008. The last glacial maximum climatic conditions on Easter
805 Island. Quaternary International 184, 166–176.

806

807 Baker, P.E., Buckley, F., Holland, J.G., 1974. Petrology and geochemistry of Easter
808 Island. Contributions to Mineralogy and Petrology 44, 85–100.

809

810 Barber, K.E., Chambers, F.M., Maddy, D., 2003. Holocene palaeoclimates from peat
811 stratigraphy: macrofossil proxy climate records from three oceanic raised bogs in
812 England and Ireland. Quaternary Science Reviews 22, 521–539.

813

814 Bennett K. D., 2002. Doucmentation for PSIMPOLL v. 4. 10 and PSCOMB V.1.03. c
815 programs for plotting pollen diagrams and analyzing pollen data.
816 http://www.chrono.qub.ac.uk/psimpoll/psimpoll.html/

817

818 Biester H, Hermanns Y-M, Martínez Cortizas A. 2012. The influence of organic
819 matter decay on the distribution of major and trace elements in ombrotrophic mires - a

820 case study from the Harz Mountains. Geochimica Cosmochimica Acta 84, 126-136.
821
822 Birks, H. H., Birks, H. J. B., 2006. Vegetation History and Archaeobotany 15, 235-
823 251.
824
825 Brown, F. B. H. 1935. Flora of Southeastern Polynesia, Vol. 3. Bernice P. Bishop
826 Museum Bulletin 130, 1-386.
827
828 Butler, K., Prior, C.A., Flenley, J.R., 2004. Anomalous radiocarbon dates from Easter
829 Island. Radiocarbon 46, 395–405.
830
831 Buurman, P., Nierop, K. G. J., Pontevedra-Pombal, X., & Martínez Cortizas, A.,
832 2006. Molecular chemistry by pyrolysis–GC/MS of selected samples of the Penido
833 Vello peat deposit, Galicia, NW Spain. Developments in Earth Surface Processes 9,
834 217-240.
835
836 Chambers F. M., Charman D. J., 2004. Holocene environmental change:
837 contributions from the peatland archive. The Holocene 14:1–6
838
839 Cañellas-Boltà N, Rull V, Sáez A, Margalef O, Bao R, Pla-Rabes S, Blaauw M,
840 Valero-Garcés B, Giralt S. 2013. Vegetation changes and human settlement of Easter
841 Island during the last millennia: a multiproxy study of the Lake Raraku sediments.
842 Quaternary Science Reviews 72, 36-48.
843
844 Cañellas-Boltá, N., Rull, V., Sáez, A., Margalef, O., Giralt, S., Pueyo, J.J., Birks,

H.H., Birks, H.J.B., Pla-Rabes, S., 2012. Macrofossils in Raraku Lake (Easter Island) integrated with sedimentary and geochemical records: towards a paleoecological synthesis. Quaternary Science Reviews 34, 113–126

Chesworth, W., Cortizas, A. M., & García-Rodeja, E.; 2006. The redox-pH approach to the geochemistry of the Earth's land surface, with application to peatlands. Developments in Earth surface processes, 9, 175-195.

Clement, A.C., Peterson, L.C.; 2008. Mechanisms of abrupt climate change of the last glacial period. Reviews of Geophysics 46 (4).

Clymo, R. S. 1984. The limits to peat bog growth. Philosophical Transactions of the Royal Society of London B 303, 605-654.

Damman A. W. H., Tolonen, K., Salanus, T., 1992. Element retention and removal in the ombrotrophic peat of Hadekeias, a boreal Finnish peat bog, Suo 43, 137-145.

Danzeglocke, U., Jöris, O., Weninger, B. 2008. CalPal-2007 online. http://www.calpal-online.de/ accessed 2009.05.03.

Desta Fekedulegn, B., JJ Colbert, RR Hicks, ME Schuckers. 2002. Coping with multicollinearity: an example on application of principal components regression in dendroecology. USDA Forest Service, Northeastern Research Station, Research Paper NE-721, 45 pp.

Dickinson, W.R., 2001. Paleoshoreline record of relative Holocene sea levels on Pacific islands. Earth-Science Reviews 55, 191–234.

Dommain, R., Couwenberg, J., Joosten, H., 2011. Development and carbon sequestration of tropical peat domes in south-east Asia: links to post-glacial sea-level changes and Holocene climate variability. Quaternary Science Reviews 30 (7–8), 999–1010.

Dransfield, J., Flenley, J.R., King, S.M., Harkness, D.D., Rapu, S., 1984. A recently extinct palm from Easter Island. Nature 312, 750–752.

Dubois, A., Lenne, P., Nahoe, E., Rauch, M., 2013. Plantas de Rapa Nui. Guía Ilustrada de la Flora de Interés Ecológico y Patrimonial. Umanga mo te Natura, CONAF, ONF International, Santiago, 132 pp.

Dumont, H.J., Cocquyt, C., Fontugne, M., Arnold, M., Reyss, J.-L., Bloemendal, J., Oldfield, F., Steenbergen, C.L.M., Korthals, H.J., Zeeb, B.A., 1998. The end of moai quarrying and its effect on Raraku Lake, Easter Island. Journal of Paleolimnology 20, 409–422

Faegri, K., Iversen, J., 1989. Textbook of Pollen Analysis, 4th Edition. Wiley, Chichester.

Flenley, J.R., King, S.M. 1984. Late Quaternary pollen records from Easter Island. Nature 307, 47–50.

Flenley, J.R., King, S.M., Jackson, J., Chew, C., Teller, J.T., Prentice, M.E., 1991. The Late Quaternary vegetational and climatic history of Easter Island. Journal of Quaternary Science 6 (2), 85-115.

Gälman V, Rydberg J, Shchukarev A, Sjöberg S, Martínez-Cortizas A, Bindler R, Renberg I. 2009. The role of iron and sulfur in the visual appearance of lake sediment varves. Journal of Pelolimnology 41, 141-153.

García-Rodeja E, Nóvoa JC, Pontevedra X, Martínez-Cortizas A, Buurman P. 2007. Aluminium and iron fractionation of European volcanic soils by selective dissolution techniques. In O Arnalds, F Bartoli, P Buurman, H Óskarsson, G Stoops, E García-Rodeja (eds) "Soils of volcanic regions in Europe", 326-351.

González-Ferran, O., Mazzuoli, R., Lahsen, A., 2004. In: Centro de Estudios Volcanológicos (Ed.), Geoloía del Complejo Volcánico Isla de Pascua Rapa Nui Santiago-Chile.1:30.000 Geol. map, (in Spanish).

Gorham, E., 1991. Northern peatlands: role in the carbon cycle and probable response to climatic warming. Ecological Applications 1, 182–195.

Gorham, E., Janssens, J.J., 2005. The distribution and accumulation of chemical elements in five peat cores from the mid-continent to the eastern coast of North America. Wetlands 25 (2) 259-278.

Gossen, C. 2007. Report: The mistery lies in the Scirpus. Rapa Nui Journal 21 (2), 105-110.

Grant, K. M., Rohling, E. J., Bar-Matthew, M. Ayalon, A. Medina-Elizalde, M., Bronk Ramsey, C., Satow, Roberts, A. P., 2012. Rapid coupling between ice volume and polar temperature over the past 150 kyr. Nature 491, 744–747

Handley L.L., Austin A.T., Robinson D., Scrimgeour C.M., Raven J.A., Heaton T.H.E., Schmidt S. and Stewart G.R., 1999. The 15N natural abundance ($\delta^{15}N$) of ecosystem samples reflects measures of water availability. Functional Plant Biology, 26(2), 185-199.

Hanebuth, T., Stattegger, K., Grootes, P.M., 2000. Rapid flooding of the Sunda Shelf: a late-glacial sea-level record. Science 288, 1033–1035.

Herrera, C., Custodio, E., 2008. Conceptual hydrogeological model of volcanic Easter Island (Chile) after chemical and isotopic surveys. Hydrogeology Journal 16 (7), 1329-1348.

Hesse, M., Halbritter, H., Zetter, R., Weber, M., Buchner, R., Frosch-Radivo, A., Ulrich, S., 2009. Pollen Terminology. An illustrated handbook. Springer WienNewYork. 261 pp

Heusser, C. J., 1971.Pollen and spores of chile: modern types of the pteridophyta, gymnospermae and angiospermae. The University of Arizona press. 165 pp.

945

946 Hoeve, M. L. and Hendrikse, M. (Eds.) 1998. A study of non-pollen objects in
947 pollen slides the types as described by Dr. Bas van Geel and colleagues. Utrech.

948

949 Hong, Y. T, Jiang, H.B, Liu, T.S., Zhou, L.P., Beer, J., Li, H.D., Leng, X.T. Hong, B.,
950 Qin, X. G., 2001. Response of climate to solar forcing recorded in a 6000-year δ18O
951 time series of Chinese peat cellulose, The Holocene 10, 1–7.

952

953 Horrocks, M., Baisden, W.T., Flenley, J., Feek, D., González Nualart, L., Haoa-
954 Cardinali, S., Edmunds Gorman, T., 2012a. Fossil plant remains at Rano Raraku, Easter
955 Island's statue quarry: evidence for past elevated lake level and ancient Polynesian
956 agriculture. Journal of Paleolimnology 48 (4), 767-783.

957

958 Horrocks, M., Baisden, W.T., Nieuwoudt, M. K., Flenley, J., Feek, D., González
959 Nualart, L., Haoa- Cardinali, S., Edmunds Gorman, T., 2012b. Microfossils of
960 Polynesian cultigens in lake sediments cores from Rano Kau, Easter Island. Journal of
961 Paleolimnology 47, Issue 2, pp 185-204.

962

963 Horrocks, M., Marra, M., Baisden, W. T., Flenley, J., Feek, D., Nualart, L. G., ... &
964 Gorman, T. E., 2013. Pollen, phytoliths, arthropods and high-resolution ^{14}C sampling
965 from Rano Kau, Easter Island: evidence for late Quaternary environments, ant
966 (Formicidae) distributions and human activity. Journal of Paleolimnology, 1-16.

967

968 Ise T, Dunn AL, Wofsy SC, Moorcroft PR., 2008. High sensitivity of peat
969 decomposition to climate change through water-table feedback. Nature Geoscience 1,

763-766.

Jackson, S.T., Charman, D. (Eds.), 2010. Editorial: “Peatlands: Paleoenvironments and carbon dynamics”. Peatlands: Palaeoenvironments and Carbon dynamics. Pages News 18.1 (2010): 3-4.

Jędrysek, Mariusz-Orion, and Grzegorz Skrzypek., 2005. Hydrogen, carbon and sulphur isotope ratios in peat: the role of diagenessis and water regimes in reconstruction of past climates. Environmental Chemistry Letters 2.4, 179-183.

Kaal, J., Baldock, J. A., Buurman, P., Nierop, K. G., Pontevedra-Pombal, X., & Martínez-Cortizas, A., 2007. Evaluating pyrolysis–GC/MS and ^{13} C CPMAS NMR in conjunction with a molecular mixing model of the Penido Vello peat deposit, NW Spain. Organic geochemistry 38 (7), 1097-1111.

Kaiser, J., Lamy, F., & Hebbeln, D., 2005. A 70‐kyr sea surface temperature record off southern Chile (Ocean Drilling Program Site 1233). Paleoceanography, 20 (4).

Krachler, M., Mohl, C., Emons, H., Shotyk, W., 2002. Influence of digestion procedures on the determination of rare earth elements in peat and plant samples by USN-ICP-MS. Journal of Analytical Atomic Spectrometry 17, 844-851.

Kylander, M. E., Weiss, D. J., Martínez Cortizas, A., Spiro, B., Garcia-Sanchez R., Coles, B. J. 2005 Refining the pre-industrial atmospheric Pb isotope evolution curve in Europe using an 8000 year old peat core from NW Spain. Earth and Planetary Science

995 Letters 240, 467-485.
996
997 Kylander, M.E., Muller, J., Wüst, R.A.J., Gallagher, K., Garcia-Sanchez, R., Coles,
998 B.J., Weiss, D.J., 2007. Rare earth element and Pb isotope variations in a 52 kyr peat
999 core from Lynch's Crater (NE Queensland, Australia): proxy development and
1000 application to paleoclimate in the Southern Hemisphere. Geochimica et Cosmochimica
1001 Acta 71, 942-960.
1002
1003 Kylander, M. E., Bindler, R., Martínez Cortizas, A., Gallagher, K., Mörth, C-M,
1004 Rauch, S., 2013. A novel geochemical approach to paleorecords of dust deposition and
1005 effective humidity: 8500 years of peat accumulation at Store Mosse (the "Great Bog"),
1006 Sweden. Quaternary Science Reviews 69, 69-82.
1007
1008 Lambeck, K., Chappell, J., 2001. Sea level change through the last glacial cycle.
1009 Science 292, 679–686.
1010
1011 Lamy, F., Hebbeln, D., Wefer, G. 1998. Late Quaternary precessional cycles of
1012 terrigenous sediment input off the Norte Chico, Chile (27.5S) and palaeoclimatic
1013 implications. Palaeogeography, Palaeoclimatology, Palaeoecology 141, 233-251.
1014
1015 Leduc, G., Vidal, L., Tachikawa, K., Bard, E. 2009. ITCZ rather than ENSO
1016 signature for abrupt climate changes across the tropical Pacific? Quaternary Research
1017 72, 123-131.
1018
1019 Loisel, J., Garneau, M., Hélie, J-F., 2010, Sphagnum $\delta^{13}C$ values as indicators of

1020 palaeohydrological changes in a peat bot. The Holocene 20, 285-291.
1021
1022 Mann, D., Edwards, J., Chase, J., Beck, W., Reanier, R., Mass, M., Finney, B., Loret,
1023 J., 2008. Drought, vegetation change, and human history on Rapa Nui (Isla de Pascua,
1024 Easter Island). Quaternary Research 69, 16-28.
1025
1026 Margalef , O. Cañellas-Boltà, N., Pla-Rabes, S., Giralt, S., Pueyo, J. J., Joosten, H.,
1027 Rull, V., Buchaca, T., Hernández, A., Valero-Garcés, B. L., Moreno, A., Sáez, A. 2013 A
1028 70,000 year geochemical and palaeoecological record of climatic and environmental
1029 change from Rano Aroi peatland (Easter Island). Global and Planetary Change 108, 72-
1030 84.
1031
1032 Martínez Cortizas, A., García –Rodeja, E., Pontevedra Pombal, X., Nóvoa Muñoz, J.
1033 C., Weiss, D., Cheburkin, A., 2002. Atmospheric Pb deposition in Spain during the last
1034 4600 years recorded by two ombrotrophic peat bogs and implications for the use of peat
1035 as archive. The Science of the Total Environtment 292, 33-34.
1036
1037 Martínez Cortizas A, Biester H, Mighall T, Bindler R. 2007a. Climate-driven
1038 enrichment of pollutants in peatlands. Biogeosciences 4, 905-911.
1039
1040 Martínez-Cortizas, A., Nóvoa, J. C., Pontevedra, X., Taboada, T., García-Rodeja, E.,
1041 & Chesworth, W. 2007b. Elemental composition of reference European volcanic soils.
1042 In *Soils of Volcanic Regions in Europe* Springer Berlin Heidelberg, pp. 289-306.
1043
1044 Meyers P.A. and Ishiwatari R. 1993. Lacustrine organic geochemistry – an overview

of indicators of organic matter sources and diagenesis in lake sediments. Org. Geochem. 20: 867–900.

Meyers, P. A. 1994. Preservation of elemental and isotopic source identification of sedimentary organic matter. Chemical Geology 114, 289-302.

Meyers, P. A, 2003. Applications of organic geochemistry to paleolimnological reconstructions: a summary of examples from the Laurentian Great Lakes. Organic Geochemistry 34, 261-289.

Moore P.D.; Webb, J.A.; & Collinson, M.E., 1991. Pollen Analysis. Blackwell Scientific Publications.

Muller, J., 2006. Reconstructing climate change of the last 55 kyr: The Lynch's Crater peat mire record, NE-QLD, Australia. PhD thesis, James Cook University

Muller, J., Kylander, M.E., Wüst, R.A., Weiss, D.J., Martinez Cortizas, A., LeGrande, N., Jennerjahn, T., Behling, H., Anderson, W. T., Jacobson, G. 2008. Possible evidence for wet Heinrich phases in tropical NE Australia: the Lynch's Crater deposit. Quaternary Science Reviews, 27(5), 468-475.

Novák, M., Wieder, R. K., & Schell, W. R., 1994. Sulfur during early diagenesis in Sphagnum peat: Insights from $\delta^{34}S$ ratio profiles in ^{210}Pb-dated peat cores. Limnology and Oceanography, 39, 1172-1172.

Novák, M., Buzek, F., Adamová, M., 1999. Vertical trends in $\delta^{13}C$, $\delta^{15}N$, $\delta^{34}S$ ratios in bulk Sphagnum peat. Soil Biology and Biochemistry 31, 1343-1346.

Orliac, C. 2000. The woody vegetation of Easter Island between the early 14th and the mid-17th Centuries A.D. in Easter Island Archaeology: Research on Early Rapanui Culture, Stevenson, C., Ayres, W. (Eds.), Easter Island Foundation, Los Osos.

Orliac, C., Orliac, M., 1998. The disappearance of Easter Island's forest: overexploitation or climatic catastrophe? In Easter Island in Pacific Context: South Seas Symposium : Proceedings of the Fourth International Conference on Easter Island and East Polynesia., Stevenson, C., Lee, G., Morin, F.J. (Eds.) Easter Island Foundation, Los Osos, pp. 129–134.

Page, S., Wüst, R., Banks, C., 2010. Past and present carbon accumulation and loss in Southeast Asian peatlands. PAGES News, 18, 1, 25-26.

Pena, L. D., Cacho, I., Ferretti, P. and Hall, M. A. 2008. El Niño–Southern Oscillation–like variability during glacial terminations and interlatitudinal teleconnections, Paleoceanography, 23.

Peteet, D., Beck,W., Ortiz, J., O'Connell, S., Kurdyla, D., Mann, D., 2003. Rapid vegetational and sediment change from Rano Aroi crater, Easter Island. Easter Island. In: Loret, J., Tanacredi, J.T. (Eds.), Scientific exploration into the world's environmental problems in microcosm. Kluwer Academic/Plenum Publ., New York, pp. 81–92.

Peterson, L. C., Haug, G. H., Hughen, K. A., and Rohl, U., 2000. Rapid changes in the hydrologic cycle of the tropical Atlantic during the last glacial, Science 290, 1947–1951.

Reille, M., 1992. Pollen et spores d'Europe et d'Afrique du Nord. Laboratoire de Botanique historique et Palynologie. Marseille, 1992. 520 pp.

Reimer, P.J., Baillie, M.G.L, Bard, E., Bayliss, A., Beck, J.W., Bertrand, C.J.H, Blackwell, P.G., Buck, C.E., Burr, G.S., Cutler, K.B., Damon, P.E., Edwards, R.L., Fairbanks, R.G., Friedrich, M., Guilderson, T.P., Hogg, A.G., Hughen, K.A., Kromer, B., McCormac, G., Manning, S., Ramsey, C.B., Reimer, R.W., Remmele, S., Southon, J.R., Stuiver, M., Talamo, S., Taylor, F.W., van der Plicht, J., Weyhenmeyer, C.E., 2004. IntCal04 terrestrial radiocarbon age calibration, 0–26 cal kyr BP. Radiocarbon 46, 1029-1058

Reimann, C., Filzmoser, P., Garrett, R. G., & Dutter, R., 2008. Principal Component Analysis (PCA) and Factor Analysis (FA). *Statistical Data Analysis Explained: Applied Environmental Statistics with R*, 211-232.

Rull, V., Cañellas-Boltà, N., Sáez, A., Giralt, S., Pla, S., Margalef, O., 2010a. Paleoecology of Easter Island: evidence and uncertainties. Earth-Science Reviews 99, 50–60.

Rull, V., Stansell, N. D., Montoya, E., Bezada, M., and Abbott, M. B. 2010b Palynological signal of the Younger Dryas in tropical Venezuelan Andes. Quaternary

Science Reviews 29, 3045–3056

Sáez, A., Valero-Garcés, B., Giralt, S., Moreno, A., Bao, R., Pueyo, J.J., Hernández, A., Casas, D. 2009. Glacial to Holocene climate changes in the SE Pacific. The Raraku Lake sedimentary record (Easter Island, 27°S). Quaternary Science Reviews 28, 2743–2759.

Schellekens, J., & Buurman, P., 2011. *n*-Alkane distributions as palaeoclimatic proxies in ombrotrophic peat: The role of decomposition and dominant vegetation. Geoderma, *164* (3), 112-121.

Schuetz L., 1989. Atmospheric mineral dust - Properties and source markers in Paleoclimatology and Paleometeorology: Modern and Past Patterns of Global Atmospheric Transport, M. Leinen & M Sarthein (Eds) NATO ASI Series, Volume 282, 359-383.

Shotyk, W., 1996. Peat bog archives of atmospheric metal deposition: geochemical evaluation of peat profiles, natural variations in metal concentrations, and metal enrichment factors. Environmental Reviews, 4(2), 149-183.

Shotyk, W., Weiss, D., Kramers, J.D., Frei, R., Cheburkin, A.K., Gloor, M., Reese, S., 2001. Geochemistry of the peat bog at Etang de la Gruère, Jura Mountains, Switzerland, and its record of atmospheric Pb and lithogenic trace metals (Sc, Ti, Y, Zr, and REE) since 12,370 14C yr BP, Geochimica et Cosmochimica Acta, 65 2337– 2360.

1145 Shotyk W, Krachler M, Martínez-Cortizas A, Cheburkin A, Emons H., 2002. A peat
1146 bog record of natural, pre-anthropogenic enrichments of trace elements in atmospheric
1147 aerosols since 12370 ^{14}C yr BP, and their variation with Holocene climate change. Earth
1148 and Planetary Letters 199, 21-37.
1149
1150 Steinmann P, Shotyk W., 1997. Chemical composition, pH, redox state of sulfur and
1151 iron in complete vertical porewater profiles from two Sphagnum peat bogs, Jura
1152 Mountains, Switzerland. Geochimica Cosmochimica Acta 62, 1143-1163.
1153
1154 Stuut, J. B., Lamy, F., 2004. Climate variability at the southern boundaries of the
1155 Namib (southwestern Africa) and Atacama (northern Chile) coastal deserts during the
1156 last 120000 yr. Quaternary Research 62, 301-309.
1157
1158 Succow, M., Joosten, H. 2001. Landschaftsökologische Moorkunde. Stuttgart,
1159 Sweizerbart, 622 pp
1160
1161 Talbot, M.R., Johannessen, T., 1992. A high resolution palaeoclimatic record for the
1162 last 27,500 years in tropical West Africa from the carbon and nitrogen isotopic
1163 composition of lacustrine organic matter. Earth and Planetary Science Letters 110, 23–
1164 37.
1165
1166 Talbot, M.R. 2001, Nitrogen isotopes in palaeolimnology in: Tracking environmental
1167 change using lake sediments. Volume 2. Physical and geochemical methods, W.M. Last
1168 and J.P. Smol (Eds.), Kluwer Academic Press, Dordrecht , pp. 401-439.
1169

1170 Tillman, P. K., Holzkämper, S., Kuhry, P., Sannel, A. B. K., Loader, N. J., Robertson,
1171 I., 2010. Stable carbon and oxygen isotopes in Sphagnum fuscum peat from subarctic
1172 Canada: Implications for palaeoclimate studies. Chemical Geology 270, 216-226.
1173
1174 Tryon, A. F., Lugardon., 1991. Spores of the Pteridophyta. Springer-Verlag New
1175 York.
1176
1177 Wang, X., Auler, A. S., Edwards, R. L., Cheng, H., Ito, E., Wang, Y., Kong, X.,
1178 Solheid, M., 2007. Millennial-scale precipitation changes in southern Brazil over the
1179 past 90,000 years, Geophysical Research Letters, 34, 1-5.
1180
1181 Weiss, D., Shotyk, W., Rieley, J.O., Page, S.E., Gloor, M., Reese, S., Cortizas-
1182 Martínez, A., 2002. The geochemistry of major and selected trace elements in a forested
1183 peat bog, Kalimantan, SE Asia, and its implications for past atmospheric dust
1184 deposition. Geochimica et Cosmochimica Acta 66, 2307–2323.
1185
1186 Whitlock, C. and Larsen,C., 2001. Charcoal as afire proxy. In: Smol J.P., Birks,
1187 H.J.B. and Last, W.M. (Eds.), Tracking environmental change using lake sediments. Vol.
1188 3: Terrestrial, algal, and siliceous indicators. Kluwer, Dordrecht, pp. 75-98.
1189
1190 Wieder, R. K., & Lang, G. E., 1988. Cycling of inorganic and organic sulfur in peat
1191 from Big Run Bog, West Virginia. *Biogeochemistry*, *5*(2), 221-242.
1192
1193 Yafa C, Farmer JG, Bacon JR, Bindler R, Renberg I, Cheburkin A, Martinez Cortizas
1194 A, Dolgopolova A, Emons H, Krachler M, Shotyk W, Li XD, Norton SA, Pulford ID,

Schweyer J, Kylander ME, Steinnes E, Weiss DJ, 2004. Development of a new ombrotrophic peat bog (low ash) reference material for the determination of elemental content. Journal of Environmental Monitoring 6:493-501.

Zizka, G., 1991. Flowering plants of Easer Island. Palmarum Hortus Francofurtensis Scientific Reports, 3, 1–108.

Zoltai SC, Johnson JD. 1985. Development of a treed bog island in a minerotrophic fen. Canadian Journal of Botany, 63, 1076-1085.